

AFML-TR-65-231, PART II

AD0649869

OFFICIAL FILE COPY

THE RELATIONSHIPS BETWEEN POLYMERS AND GLASS TRANSITION TEMPERATURES

O. G. Lewis
L. V. Gallacher
American Cyanamid Company

TECHNICAL REPORT AFML - TR - 65 - 231, PART II

JULY 1966

AIR FORCE MATERIALS LABORATORY
RESEARCH AND TECHNOLOGY DIVISION
AIR FORCE SYSTEMS COMMAND
WRIGHT-PATTERSON AIR FORCE BASE, OHIO

20040219339

Best Available Copy

NOTICES

When Government drawings, specifications, or other data are used for any purpose other than in connection with a definitely related Government procurement operation, the United States Government thereby incurs no responsibility nor any obligation whatsoever; and the fact that the Government may have formulated, furnished, or in any way supplied the said drawings, specifications, or other data, is not to be regarded by implication or otherwise as in any manner licensing the holder or any other person or corporation, or conveying any rights or permission to manufacture, use, or sell any patented invention that may in any way be related thereto.

Qualified requesters may obtain copies of this report from the Defense Documentation Center (DDC), (formerly ASTIA), Cameron Station, Bldg. 5, 5010 Duke Street, Alexandria, Virginia, 22314.

This report has been released to the Office of Technical Services, U.S. Department of Commerce, Washington 25, D. C., for sale to the general public.

Copies of this report should not be returned to the Research and Technology Division, Wright-Patterson Air Force Base, Ohio, unless return is required by security considerations, contractual obligations, or notice on a specific document.

THE RELATIONSHIPS BETWEEN POLYMERS AND

GLASS TRANSITION TEMPERATURES

O. G. Lewis
L. V. Gallacher
American Cyanamid Company

July 1966

Distribution of this document is unlimited.

Best Available Copy

FOREWORD

This report was prepared by the Central Research Division of American Cyanamid Company, Stamford, Connecticut, under USAF Contract No. AF 33(657)-11224. The contract was initiated under Project No. 7342, "Fundamental Research on Macromolecular Materials and Lubrication Phenomena," Task No. 734203, "Fundamental Principles Determining the Behavior of Macromolecules." It was administered under the direction of the Air Force Materials Laboratory, Research and Technology Division, with Dr. Ivan Goldfarb as project engineer.

This report covers work conducted from June 1965 to May 1966. The authors are indebted to Professor J.H. Gibbs for helpful discussions. The assistance of R. Maurice King, K. F. Kolb, and A. I. Weiss in the mathematical analysis is gratefully acknowledged.

The manuscript was released by the authors 9 September 1966 for publication as an R & D Technical Report.

This technical report has been reviewed and is approved.

William E. Gibbs

William E. Gibbs
Chief, Polymer Branch
Nonmetallic Materials Division
Air Force Materials Laboratory

ABSTRACT

The glass transition is an experimental manifestation of the extremely large activation energies for molecular motion encountered as the temperature of a liquid is lowered. As an approach to the effect of molecular structure on this phenomenon, low-shear melt viscosities were obtained as a function of temperature for three homologous series of polymers: polypropylene, poly(chlorotrifluoroethylene) and poly(propylene oxide). The data are well represented by an equation arising from the Adam-Gibbs theory: $\log \nu = A + B/(T \ln T/T_0)$, where ν is the kinematic viscosity. The best-fit values of the parameters in this equation are as follows:

Polymer of	\bar{M}_n	A	B	T_0
Propylene	900	-1.182	841	171.6
Propylene	1210	-1.220	974	172.4
Chlorotrifluoroethylene	640	-0.982	338	164.8
Chlorotrifluoroethylene	820	-1.223	521	186.5
Chlorotrifluoroethylene	1050	-1.811	938	166.0
Propylene Oxide	460	-0.786	392	180.7
Propylene Oxide	1250	-0.336	403	177.0
Propylene Oxide	2080	-0.070	409	175.3
Propylene Oxide	3620	0.036	619	148.7

A kinetic model of the glass transition was devised for computer simulation of dilatometric behavior in the region of a transition. The assumption that the dielectric and volume relaxation times are equal was shown to be satisfactory for prediction of dilatometric results on polymers. The effects of rate of heating, activation energy and coefficients of expansion on the measurement of transitions were demonstrated.

The Gibbs-DiMarzio theory of the glass transition was cast in a form suitable for very short chains and shown to agree quantitatively with T_0 values for the lower n-alkanes. The theory was also shown to be applicable to polymer structures having chain bonds of zero flex energy. In this case, the intermolecular energy and number of lattice-site occupiers must be estimated empirically.

The Eyring transition state theory of relaxation processes was shown to be applicable to dielectric relaxation in polymers with modification to allow for a temperature-dependent activation free energy ΔG^\ddagger . A "Dielectric transition temperature" was defined as the temperature at which the relaxation time τ equals 1000 sec. It was shown that this temperature is very close to the dilatometric glass

temperature, except in poly(butyl methacrylate) where the α and β relaxations are unresolved. The ratio $\Delta G_g^\ddagger(\tau)/Tg(\tau)$ at the dielectric transition temperature was found to be 72.4 ± 0.08 cal deg⁻¹ mol⁻¹ at $\tau = 1000$ sec.

TABLE OF CONTENTS

	PAGE
1. Relationships between Molecular Structure and Melt Viscosity	1
A. Introduction	1
B. Materials	1
C. Experimental Methods	1
D. Experimental Results	6
E. Interpretation of the Experimental Data	11
2. A Kinetic Model for Dilatometric Transitions	18
3. Gibbs-DiMarzio Theory of the Glass Transition	43
A. Introduction	43
B. Flex Energy in <u>n</u> -Alkanes	43
C. Chain Bonds with Zero Flex Energy	46
4. Transition State Theory and the Glass Transition	52

TABLES

	PAGE
I. The Polymers Studied in the Melt Viscosity Program	2
II. Typical Calculated Kinetic Energy Constants for use in Equation (1)	4
III. Experimental Results	7
IV. Shear Rate Dependence of the Melt Viscosities	12
V. Least Squares Analysis of Viscosity Results	13
VI. Changes in Thermal Expansion Coefficients for PMMA and PVC in Observed Dilatometric Transitions	19
VII. Equation (47) Results and Comparison of Variance Estimates Obtained with Equations (44) and (47)	54
VIII. Transition State Parameters at the Glass Temperature Computed with Equations (48), (49) and (50)	55
IX. Values of ΔG_g^\ddagger and $\Delta G_g^\ddagger/T_g$ Computed before and after Reduction to Fixed Relaxation Time ($T_g = 10^3$ sec)	59

ILLUSTRATIONS

FIGURE NO.		PAGE
1.	Kinematic Viscosities of the Propylene Oxide Polymers	8
2.	Kinematic Viscosities of the Propylene Polymers	9
3.	Kinematic Viscosities of the Fluorocarbon Polymers	10
4.	Residual Patterns Observed with Equation (8) Using Poly(propylene Oxide) Data	15
5.	The Behavior of the Sum of the Squares as a Function of T_0 for Each of the Poly(propylene Oxides). Equation (8)	16
6.	Computed Volume-Temperature Curves for PVC Showing Glass Transition	26
7.	Computed Volume-Temperature Curves for PMMA Showing Glass Transition	27
8.	Computed Volume-Temperature Curves Showing β Transition in PMMA	28
9.	The Glass Transition in Poly(ethyl Methacrylate)	29
10.	The Glass Transition in Poly(vinyl Acetate)	30
11.	The Glass Transition in PVAc, 316 Deg./Hr., Equilibrium Relaxation Time	31
12.	The Variation of T_g with Cooling Rate, PVC	33
13.	The Variation of T_g with Cooling Rate, PMMA	34
14.	The Rate-Dependence of the β Transition in PMMA	35
15.	Linear Plot of the Variation of T_g with Cooling Rate, PMMA	36
16.	The Rate-Dependence of τ at the Transition Temperature	37
17.	Computed Relaxation Time (α Process) for PVC at Different Cooling Rates	39
18.	Computed Relaxation Time (α Process) for PMMA at Different Cooling Rates	40

- | | |
|---|----|
| 19. Computed Relaxation Time (β Process) for PMMA at Different Cooling Rates | 41 |
| 20. Calculated and Observed Transition Temperatures in <u>n</u> -Alkanes | 47 |
| 21. Variation of ΔG^\ddagger with Temperature near T_g | 57 |

1. Relationships between Molecular Structure and Melt Viscosity

A. Introduction

In order to develop a better understanding of the relationship between the glass transition and molecular structure, it is of primary importance that we first learn more about the mechanisms involved in transport processes in polymers. It is generally accepted that the experimental glass transition is a manifestation of the decrease in the rate of a specific transport process at low temperatures. Melt viscosity is a transport property that is particularly easy to measure, at least in principle. Therefore, it is not surprising that a number of theories relating melt viscosity to T_g have been proposed¹⁻⁵. Unfortunately, there has been a rather inadequate effort made to obtain reliable low-shear melt viscosity data over a wide temperature range.

With these factors in mind, we decided to make viscosity measurements on three series of low molecular weight polymers. Low molecular weights were selected for several reasons. First, shear rate effects are minimized. Second, viscosities are low enough so that capillary viscometers can be used. Third, theoretical complications arising from chain entanglements are avoided.

B. Materials

Commercially important polymers with readily available low-molecular weight homologs were chosen: poly(chlorotrifluoroethylene), polypropylene, and poly(propylene oxide). Molecular weights of all polymers were determined with a Mechrolab vapor pressure osmometer. End group analysis was used on the poly(propylene oxide) polymers as a check. The polymers are described in Table I. All measurements were performed on the polymers as received.

C. Experimental Methods

All viscometers used were suspended-level capillary instruments, including both Cannon dilution and Ubbelohde viscometers. The use of suspended-level viscometers eliminates the need for a temperature correction. All of the viscometers were calibrated with viscosity standards newly purchased from the National Bureau of Standards.

Calibrations and measurements were performed in an insulated water bath in the temperature range of 25°-90°C. The temperature of the bath was measured with a Leeds and Northrup platinum resistance thermometer and Mueller bridge. Although the thermometer was supplied with the Callendar equation constants, the combination of bridge and thermometer was recalibrated at the ice point using the procedure outlined by Robertson

TABLE I

The Polymers Studied in the Melt Viscosity Program

<u>Polymer</u>	<u>Commercial Name</u>	<u>Source</u>	<u>Number Ave. Mol. Wt.</u>
Poly(propylene Oxide)	P-400	Dow Chemical Co.	460
	P-1200	Dow Chemical Co.	1250
	P-2000	Dow Chemical Co.	2080
	P-4000	Dow Chemical Co.	3620
Polypropylene	C-60	Amoco Chemical Corp.	900
	C-175	Amoco Chemical Corp.	1210
Poly(chlorotrifluoroethylene)	FS-5	Hooker Chemical Corp.	640
	S-30	Hooker Chemical Corp.	820
	LG-160	Hooker Chemical Corp.	1050

and Walch⁶. All measurements were made after steady state conditions were obtained with a measured current through the thermometer of 2.3 milliamperes. Cycling variations in the bath did not appear to exceed $\pm 0.01^\circ\text{C}$, as measured with the platinum thermometer and a companion mercury-in-glass thermometer read with a cathetometer. Presumably, variations of fluid temperature within glass viscometers immersed in the bath would be much less, because of the long time constants for thermal equilibration of the viscometers.

The viscometer calibrations were all performed at a bath temperature of $37.80 \pm .05^\circ\text{C}$. Temperatures were read to 0.01°C and viscosities of the standards were corrected to the measurement temperature. In order to avoid calibrating the viscometers in the non-Newtonian region, the viscometers were calibrated either with a single fluid with a very long flow time (~ 500 seconds) or with several fluids having a spectrum of flow times. A minimum of three runs agreeing within 0.3 per cent (maximum) was made with each fluid.

In calibrating the viscometers, we attempted to determine the kinetic energy constants using the equation of Cannon, Manning, and Bell⁷:

$$\nu = k_1 t - k_2/t_2 \quad (1)$$

Here ν is the kinematic viscosity in centistokes, k_1 is the limiting flow-time constant, k_2 is the kinetic energy correction constant, and t is the efflux time in seconds. We discovered that it was virtually impossible to arrive at consistent values for k_2 for most of the viscometers using the ordinary method of obtaining one very low flow time to determine k_1 and one short flow time to fix k_2 . In Reference (7) the authors found a correlation between k_2 and the Reynolds number which led to an expression for k_2 in terms of k_1 and viscometer dimensions,

$$k_2 = \frac{1.66 V^{3/2}}{L (Dk_1)^{1/2}} \quad (2)$$

Here V is the efflux volume (bulb volume), L is the capillary length, and D is the capillary bore. Using this equation, Cannon, Manning and Bell were able to calculate kinetic energy constants in excellent agreement with experiment for a number of suspended level viscometers. We therefore decided to compute the kinetic energy correction constants for our viscometers from Equation (2). Since these are standard viscometers, all of the necessary dimensions can be found in ASTM manuals⁸. Typical values of the kinetic energy constants are recorded in Table II. In addition, the flow time for 0.1 per cent correction is indicated.

TABLE II

Typical Calculated Kinetic Energy
Constants for Use in Equation (1)

<u>Viscometer Type</u>	<u>Size</u>	<u>Kinetic Energy Constant</u>	<u>Time for 0.1% Correction, Seconds</u>
Cannon-Ubbelohde	75	130	243
	100	85	171
	150	54	115
	200	27	63
Ubbelohde	2C	10	33
	3C	3	10
	4	1.4	5

Since the flow times were generally in excess of the time for 0.1 per cent error, the kinetic energy correction is insignificant with all but the size 75 and size 100 viscometers.

It was also of interest in this study to determine the average shear rate for each run. If we assume that the flow is Newtonian, it is shown readily⁹ that the shear rate at a radial distance r from the center of the capillary is

$$\dot{\gamma}(r) = \frac{\Delta p r}{2\eta L}, \quad (3)$$

where

$\dot{\gamma}(r)$ is the shear rate in sec^{-1} ,
 Δp is the driving pressure,
 η is the viscosity in poises,
 L is the capillary length.

Δp is conveniently expressed as ρhg , where ρ is the liquid density, h the average head, and g the gravitational constant. The viscosity can be given as $(\rho k_1 t)/100$. Making the appropriate substitutions, we obtain

$$\dot{\gamma}(r) = \frac{50 hgr}{k_1 t L} \quad (4)$$

The maximum shear rate is formed by setting r equal to R , the capillary radius:

$$\dot{\gamma}_{\text{max.}} = \frac{50 hgR}{k_1 t L} \quad (5)$$

The average shear rate is given by

$$\dot{\gamma}_{\text{ave.}} = \frac{\int_0^R \dot{\gamma}(r) 2\pi r dr}{\int_0^R 2\pi r dr} \quad (6)$$

which leads to the result

$$\dot{\gamma}_{\text{ave.}} = \frac{100 \text{ hgR}}{3 k_1 tL} \quad (7)$$

Thus, the average shear rate is just 2/3 of the maximum value.

D. Experimental Results

The kinematic viscosities and corresponding shear rates are given in Table III. The results are shown graphically in Figures 1, 2 and 3.

When the viscosities were measured originally, the bath temperature was measured with a Fisher Scientific precision thermometer with 0.1°C graduations (catalogue No. 15-043), which was calibrated with a standard platinum resistance thermometer and Mueller bridge after the measurements were completed. The glass thermometer was read by eye, without the aid of a cathetometer. In making the more recent measurements, the bath temperatures were always measured directly with the platinum thermometer, thereby eliminating the cumulative error of two visual glass thermometer readings. A mercury-in-glass thermometer was used with a cathetometer as an aid in setting and regulating the bath temperature. A comparison of the old and new results shows an average viscosity difference of 0.9 per cent, corresponding to an average cumulative temperature error of about 0.2 degrees centigrade. We conclude that the use of platinum resistance thermometers or, at the very least, calibrated 0.1 degree mercury-in-glass thermometers and cathetometers is essential for accurate measurement of bath temperatures.

Another source of error which has been eliminated in the measurements reported in Table III is the error in shear stress resulting from deviations of the capillary from the true vertical direction. The per cent error introduced here is given by $100(1 - \cos \theta)$, where θ is the deviation from the vertical direction. A 5° deviation of the capillary gives a 0.4 per cent error. The limit for 0.1 per cent error is 2° 34'. Therefore, since we are concerned with errors in the fractional per cent range, it is desirable to eliminate this error. This has been done by setting up two viscous-damped plumb lines. When each viscometer is placed in the bath, it is adjusted so that the capillary lines up with both plumb lines. Assuming that this procedure reduces the angular deviation to less than 2°, the corresponding viscosity error is less than 0.06 per cent.

We feel, therefore, that the viscosities given in Table III are accurate to within 0.5 per cent. There may be some question as to whether or not we have actually obtained the Newtonian viscosities of

TABLE III

Experimental Results

Polymer	Temperature, °C	Time, Seconds	Viscosity, Centistokes	Kinetic Energy Correction, cs.	Average Shear Rate, sec ⁻¹
P-400	25.01	637.2	69.4	<.001	29.
	37.81	316.7	34.5	<.001	58.
	49.87	555.6	20.16	<.001	77.
	59.91	381.1	13.83	<.001	112.
	69.90	585.8	9.97	<.001	125.
	79.92	437.8	7.45	<.001	168.
	89.94	340.0	5.79	<.001	216.
Pl200	25.01	1655.7	180.1	<.001	14.6
	37.81	844.0	91.8	<.001	29.
	49.87	501.4	54.5	<.001	48.
	59.91	348.4	37.9	<.001	69.
	69.90	602.0	27.54	<.001	56.
	79.92	453.2	20.73	<.001	75.
	89.94	352.7	16.14	<.001	96.
P-2000	25.00	1125.0	324.	<.001	10.8
	37.81	577.4	166.5	<.001	21.
	49.87	943.0	99.9	<.001	25.
	59.91	657.4	69.6	<.001	36.
	69.90	478.4	50.7	<.001	49.
	79.92	360.4	38.2	<.001	65.
	89.94	829.9	29.9	<.001	52.
P-4000	25.00	363.5	1049.	<.001	6.1
	37.81	185.0	534.	<.001	12.1
	49.87	1104.6	319.	<.001	11.0
	59.91	763.6	220.1	<.001	16.
	69.90	545.5	157.3	<.001	22.
	79.92	398.1	114.8	<.001	30.
	89.94	304.7	87.8	<.001	40.
C-60	25.99	729.4	7513.	<.001	1.2
	37.79	229.8	2367.	<.001	3.7
	49.85	289.2	861.	<.001	7.5
	59.95	141.3	421.	<.001	15.
	69.93	835.9	222.6	<.001	15.
	79.91	486.5	131.9	<.001	27.
	89.96	300.7	81.5	<.001	43.
C-175	49.85	369.5	3787.	<.001	2.3
	59.95	160.5	1645.	<.001	5.3
	69.93	260.6	798.	<.001	8.1
	79.91	137.7	421.	<.001	15.
	89.96	78.2	239.	<.001	27.
FS-5	25.08	951.9	8.43	<.001	127.
	37.79	602.7	5.34	<.001	201.
	49.85	419.3	3.71	<.001	289.
	59.95	324.6	2.87	.001	373.
	69.93	259.2	2.29	.002	467.
	79.91	212.1	1.878	.003	570.
	89.96	176.4	1.561	.004	686.
S-30	25.08	1061.7	316.4	<.001	11.
	37.79	386.4	115.2	<.001	30.
	49.85	174.0	51.9	<.001	67.
	59.95	99.6	29.7	.001	117.
	69.93	517.4	18.66	<.001	83.
	79.91	342.8	12.36	<.001	125.
LG-160	25.08	344.9	3535.	<.001	2.5
	37.79	342.0	987.	<.001	6.5
	49.85	122.1	352.	<.001	18.
	59.85	586.5	169.1	<.001	21.
	69.93	309.0	89.1	<.001	39.
	79.91	175.6	50.6	<.001	69.
	89.96	106.9	30.8	<.001	113.

Figure 1

Kinematic Viscosities of the Propylene Oxide Polymers

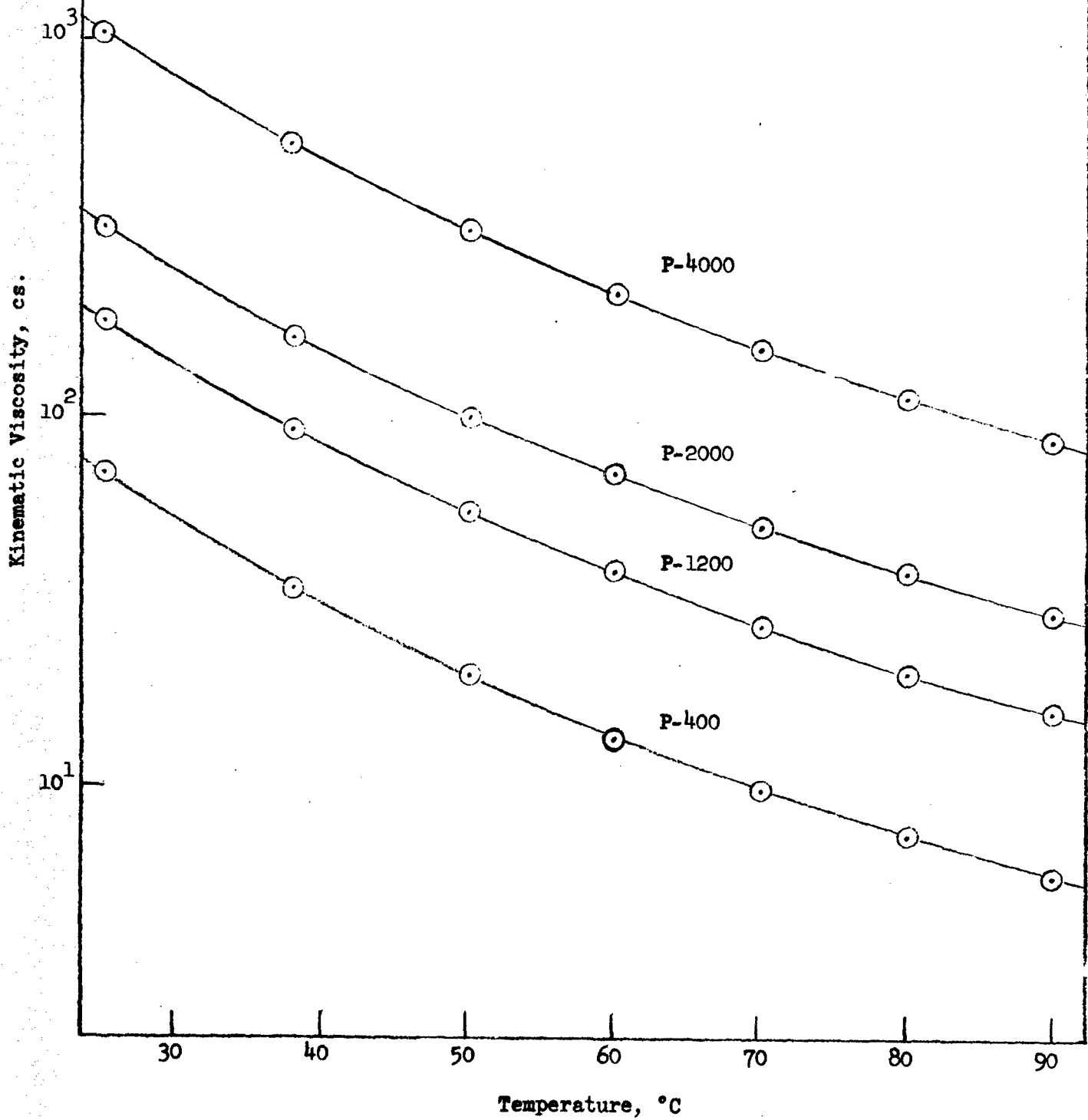


Figure 2

Kinematic Viscosities of the Propylene Polymers

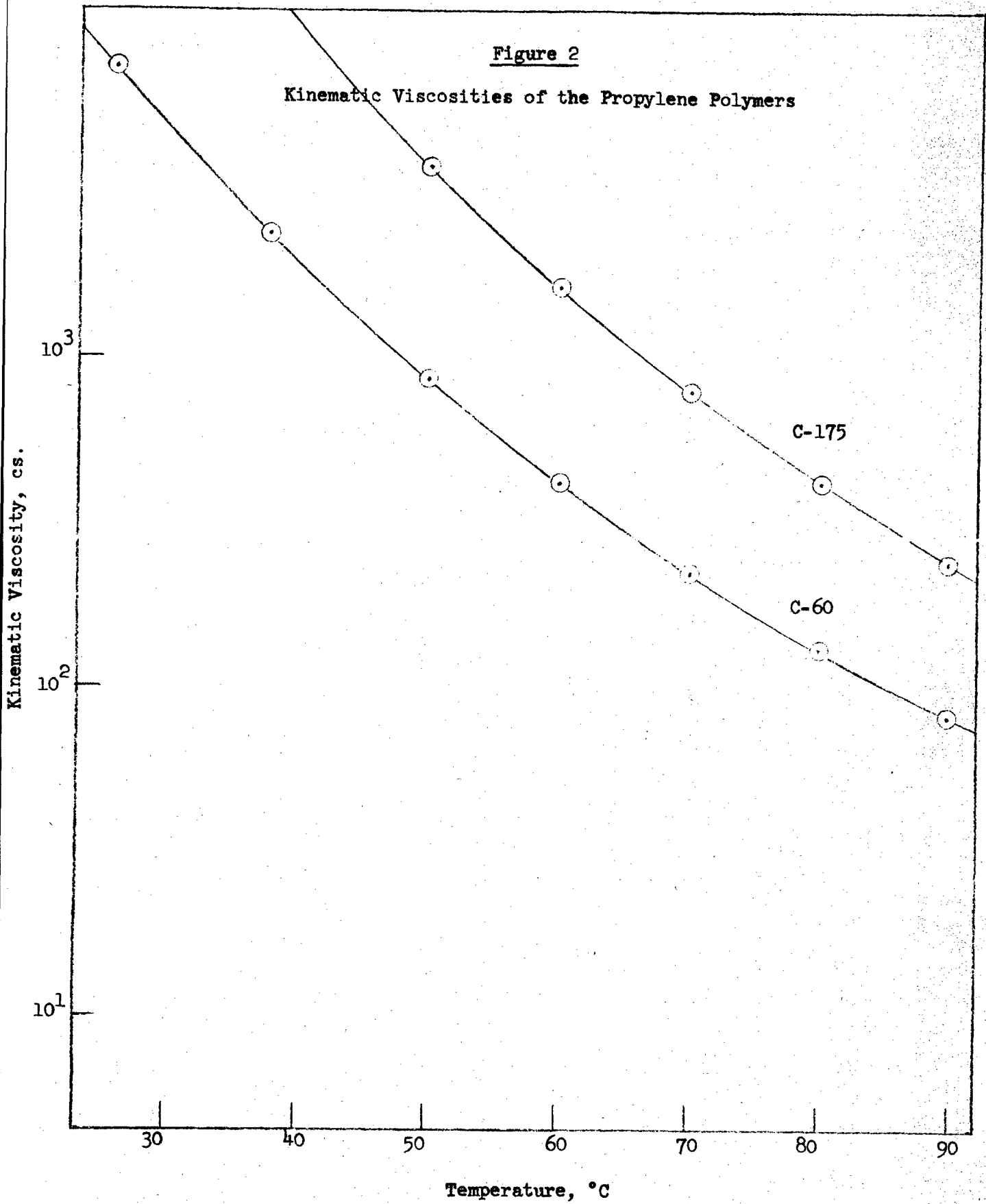
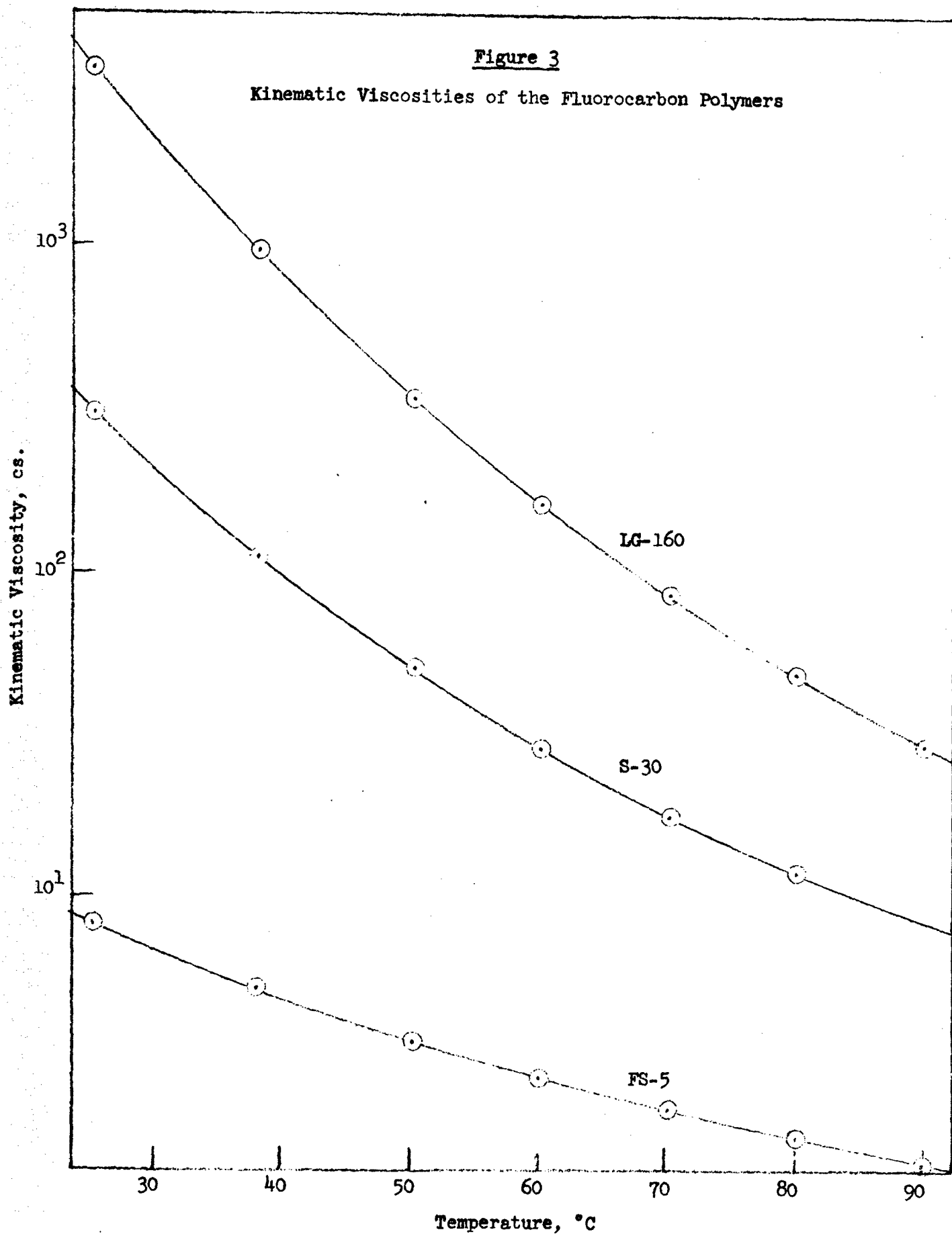


Figure 3

Kinematic Viscosities of the Fluorocarbon Polymers



these polymers. The early measurements on the polypropylene oxide polymers were made at shear rates higher by a factor of two than those reported here. Nevertheless, there is no systematic shear rate dependence visible in the data. The polypropylenes and at least one of the fluorocarbons show no significant shear-rate effects. This is shown in Table IV.

Further, one would not expect to observe significant deviations from Newtonian flow with these polymers in any case because of the low molecular weights involved. Normally, large deviations are observed only above the critical entanglement molecular weight, which is about 15,000 for polypropylene oxide and 7,000 for atactic polypropylene¹⁰.

E. Interpretation of the Experimental Data

In order to evaluate current glass transition theories, four equations were fitted to the experimental data using non-linear least squares analysis. The equations are given below:

$$\log \nu = A + \frac{B}{T-T_0}, \quad (8)$$

$$\log \nu = A - \log T + \frac{B}{T-T_0}, \quad (9)$$

$$\log \nu = A + \frac{B}{T \ln T/T_0}, \quad (10)$$

$$\log \nu = A - \log T + \frac{B}{T \ln T/T_0}. \quad (11)$$

All four equations require kinematic viscosity data. In addition, absolute viscosities were obtained for the poly(propylene oxide) polymers by utilizing the density-temperature relationship reported by Baur and Stockmayer⁷. Equation (8) is a form of the empirical Fulcher equation¹¹, which has received considerable theoretical support in recent years^{1,2}. Equation (9) is an adaptation of transition state theory which provides a temperature dependent ΔG^\ddagger . Equations (10) and (11) are both based upon the Adam-Gibbs⁴ equation. Further discussion of these equations can be found in this report and the preceding summary report⁵.

The results of the least-squares analyses are given in Table V. Variance estimates for each computation are included in the table.

TABLE IV

Shear Rate Dependence of the Melt Viscosities

<u>Polymer Designation</u>	<u>Temperature</u>	<u>Viscosity, cs.</u>	<u>Average Shear Rate, sec⁻¹</u>
C-60 (polypropylene)	69.93	226.6	15.4
		226.2	28.
C-175 (polypropylene)	69.93	798.	8.1
		798.	10.9
		421.	15.
		421.	21.
S-30 (chlorotrifluoroethylene)	69.93	18.7	83.
		18.5	189.

TABLE V

Least Squares Analysis of Viscosity Results

Polymer	Equation*	A	B	T ₀	Variance Estimate x 10 ⁵
Polypropylene (C-60)	8	-1.718	659	181.4	1.31
	9	1.136	590	186.2	1.55
	10	-1.182	841	171.6	1.02
	11	1.628	739	177.4	1.23
Polypropylene (C-175)	8	-1.791	748	183.8	0.95
	9	1.093	670	189.0	1.11
	10	-1.220	974	172.4	0.73
	11	1.616	856	178.6	0.87
Polychlorotrifluoroethylene (FS-5)	8	-1.188	259	175.7	0.13
	9	1.670	188	189.5	0.11
	10	- .982	338	164.8	0.15
	11	1.829	333	181.3	0.11
Polychlorotrifluoroethylene (S-30)	8	-1.603	430	193.6	1.16
	9	1.214	374	198.9	1.34
	10	-1.223	521	186.5	1.00
	11	1.552	446	192.7	1.17
Polychlorotrifluoroethylene (LG-160)	8	-2.388	723	176.6	1.39
	9	0.476	649	181.3	1.63
	10	-1.811	938	166.0	1.07
	11	1.006	827	171.7	1.28
Poly(propylene oxide) P-400	8	-1.053	316	189.0	0.13
	9	1.781	255	197.6	0.23
	10	-0.786	392	180.7	0.15
	11	2.005	308	190.8	0.15
Poly(propylene oxide) P-1200	8	-0.604	321	185.8	0.19
	9	2.237	258	194.9	0.14
	10	-0.336	403	177.0	0.29
	11	2.461	313	187.7	0.16
Poly(propylene oxide) P-2000	8	-0.339	324	184.4	0.08
	9	2.505	259	193.6	0.07
	10	-0.070	409	175.3	0.11
	11	2.729	317	186.2	0.07
Poly(propylene oxide) P-4000	8	-0.299	450	162.6	1.38
	9	2.591	365	172.6	1.24
	10	0.036	619	148.7	1.52
	11	2.876	481	161.1	1.36
Poly(propylene oxide) P-400	8a	-1.366	380	179.6	0.059
	9a	1.489	310	188.3	0.035
	10a	-1.058	487	169.6	0.094
	11a	1.751	386	179.9	0.050
Poly(propylene oxide) P-1200	8a	-0.925	389	175.9	0.12
	9a	1.937	316	185.0	0.07
	10a	-0.616	506	165.1	0.17
	11a	2.200	397	176.0	0.10
Poly(propylene oxide) P-2000	8a	-0.663	393	174.2	0.15
	9a	2.203	319	183.4	0.10
	10a	-0.353	515	163.0	0.20
	11a	2.465	403	174.2	0.14
Poly(propylene oxide) P-4000	8a	-0.680	546	150.6	1.64
	9a	2.235	448	160.6	1.50
	10a	-0.297	793	133.6	1.79
	11a	2.565	621	146.2	1.64

* Equation numbers correspond to those in text. Numbers followed by "a" indicate the use of absolute viscosity in the equation.

In general the fits were excellent, with a range of variance estimates for $\log \eta$ and $\log \nu$ of 4×10^{-7} to 1.7×10^{-5} . Closer examination indicated that there were persistent trends in the residual patterns obtained for the poly(propylene oxides), but not in those obtained for the other polymers. Figure 4 illustrates this. It can be seen in the figure that at any given temperature the residuals increase with molecular weight, with the P-4000 residuals generally several times larger than the others. At first it was thought that this might be the result of small temperature errors coupled with activation energies increasing with molecular weight. The residual for the P-4000 polymer at 37.8°C is in fact equivalent to a temperature error of 0.23°C , as calculated with an equation easily derived from Equation (8):

$$\Delta T \approx \frac{\Delta \log \nu (T-T_0)^2}{B} . \quad (12)$$

ΔT values for P-400, P-1200, and P-2000 at 37.8 turn out to be equal to $< 0.01^\circ\text{C}$, 0.04°C , and 0.05°C respectively. These values are inconsistent with the notion that the residual pattern was caused by temperature errors, since all of these polymers were run consecutively at each temperature in the same bath. When the activation energies of the four poly(propylene oxides) were calculated at 37.8°C using the constants from Equation (8)

$$E_\nu = 2.303 RB \left(\frac{T}{T-T_0} \right)^2 , \quad (13)$$

it was found that the energies for all four polymers were equal to within four per cent. Therefore, the molecular weight trend evident in Figure 4 cannot be attributed to temperature error.

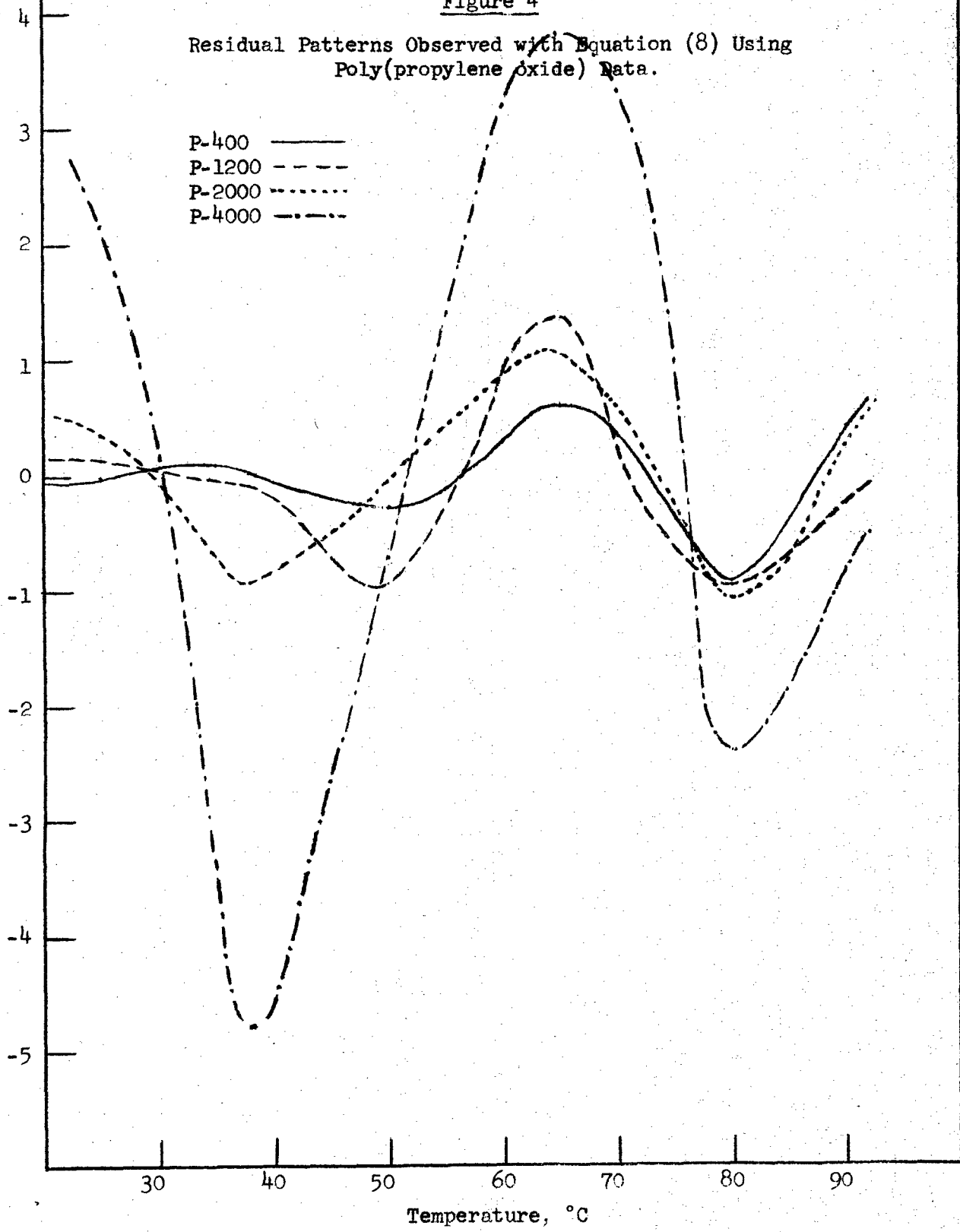
The next factor to be considered was the dependence of the sum of the squares upon the choice of T_0 for each polymer. This dependence is shown in Figure 5 for Equation (8), which gave results comparable to the other equations. It is evident from the figure that a relatively poor fit was obtained with the P-4000 data. The relative dispersion in the sum of the squares for P-4000 is much larger than for the other polymers. This is in line with the residual pattern in Figure 4. This sort of behavior can result either from errors in the experimental data points or simply from model failure. The definite residual pattern makes error seem unlikely as the source of the problem; thus, we are left with model failure. Analysis of the results given in Figure 4 reveals that this sort of pattern results from the use of a function having inadequate curvature at low temperatures

Figure 4

Residual Patterns Observed with Equation (8) Using Poly(propylene oxide) Data.

P-400 ———
P-1200 - - - -
P-2000 ·····
P-4000 - · - ·

Residual x 10³



Sum of the Squares $\times 10^5$

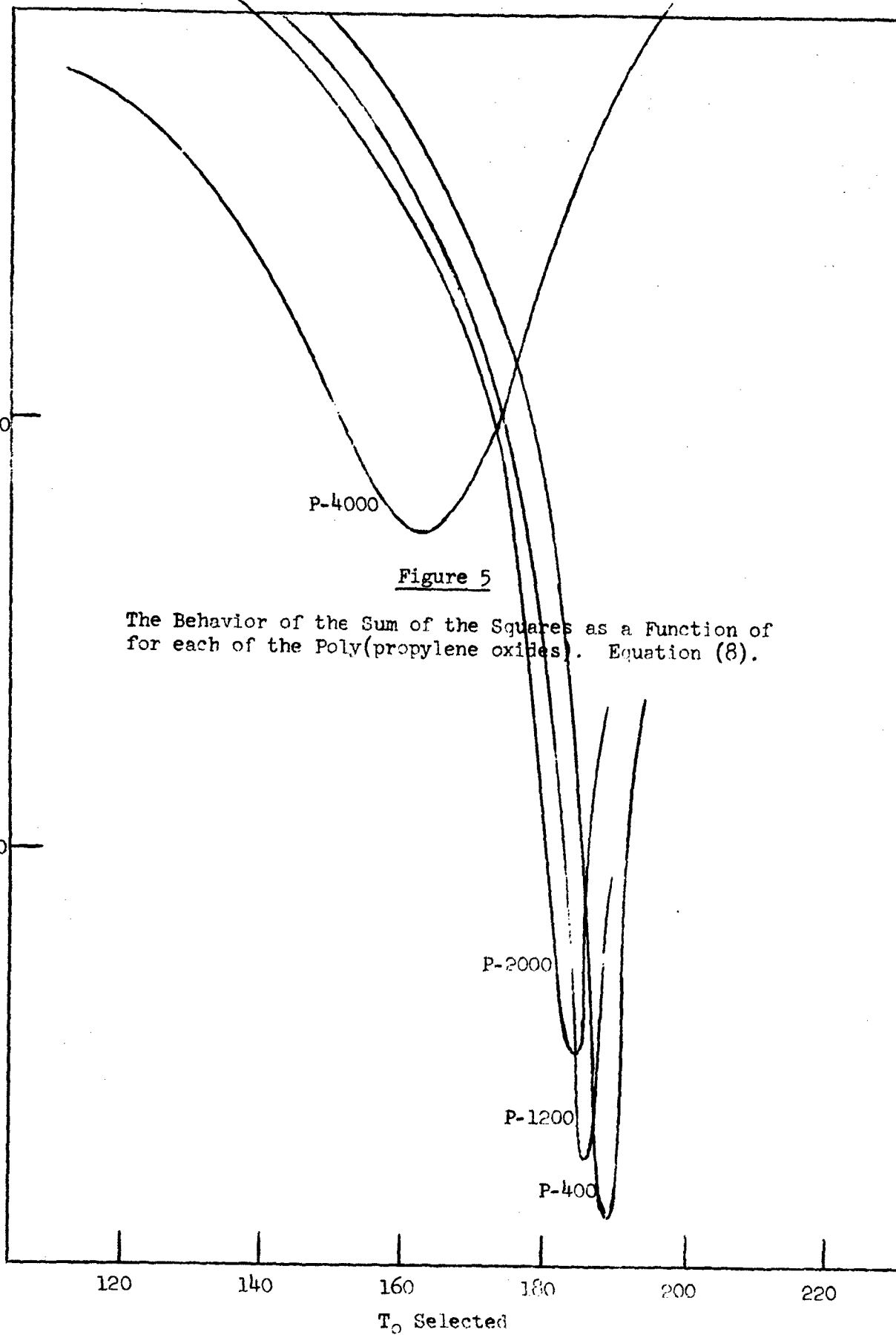


Figure 5

The Behavior of the Sum of the Squares as a Function of for each of the Poly(propylene oxides). Equation (8).

and high temperatures, and too much curvature in the intermediate temperature range. Each of the Equations (8) through (11) gave the same over-all pattern with no equation offering a large advantage over the others. However, the residuals were so small in every case that all of the equations looked very good.

In the next phase of this work, the molecular theories corresponding to Equations (8) through (11) will be critically evaluated using the results published herein. It is obvious that goodness-of-fit by itself is not an adequate criterion for judging a theory, since all four equations give comparable results with our data. The real tests lie in the ability to predict reasonable molecular structural parameters with each equation, and in the consistency of these predictions within a given polymer series.

2. A Kinetic Model for Dilatometric Transitions

Recently, a number of publications have appeared reporting the observation of dilatometric or specific heat transitions in amorphous polymers below the glass transition temperature¹²⁻¹⁵. Heretofore, it was believed by many that only the glass transition would be observed in such measurements. Many textbooks in fact define the glass transition temperature as that temperature where the expansion coefficient of an amorphous polymer is discontinuous, implying that this change is unique. Virtually all published theories of the glass transition consider only one amorphous transition.

Actually, it appears to be quite reasonable to expect dilatometric transitions below T_g . Dynamic mechanical and dielectric measurements invariably indicate one or more loss regions below that attributed to the glass transition^{16,17}. Furthermore, relaxation times observed in these measurements point to the existence of transitions near those found recently in dilatometric or specific heat experiments.

For example, Saito¹⁶ indicates a one cycle dielectric loss peak for poly(vinyl chloride) (PVC) at -38°C . Heydemann and Guicking¹² report a dilatometric transition at -26°C . Dilatometric transitions in poly(methyl methacrylate) (PMMA) around 0°C have been reported by Heydemann and Guicking¹² and by Holt and Edwards¹⁵. Saito's¹⁶ results show a one cycle loss peak at 0°C .

The rate dependence of the specific heat glass transition temperature has been demonstrated effectively by Wunderlich and Bodily¹⁸. If the secondary transitions are also rate-dependent, it should be possible to characterize this dependence in terms of a temperature-dependent relaxation time and the experimental time scale. Also, it should be possible to determine the factors which make a transition more or less discernible.

A large activation energy will compress the temperature region in which the relaxation time is of the order of the experimental time scale, thus sharpening the observed transition. The activation energy for the α relaxation process (the process resulting in the glass transition) generally increases with decreasing temperature; thus, a simple Arrhenius equation will not fit viscosity or dynamic data. This sort of behavior can be described adequately by the WLF equation¹, which yields for the activation energy at the glass temperature

$$E_g = \frac{2.303 RC_1 \epsilon T_g^2}{C_2 \epsilon} \quad (14)$$

Here R is the gas constant and C_1g and C_2g are the WLF parameters for a reference temperature of T_g obtained by fitting experimental data. E_g values calculated with Equation (14) range from 50 to about 200 kcal. per mole. Values obtained by using the Arrhenius equation well above the glass temperature are usually lower. The evidence obtained from dynamic measurements of low temperature relaxation processes indicates that these processes exhibit an Arrhenius temperature dependence^{16,19}. Activation energies are generally lower than 30 kcal. per mole^{16,20,21}. Therefore, it is reasonable to expect secondary transitions to be much broader and more difficult to resolve than the glass transition.

A broad distribution of relaxation times will broaden a transition region since it gives rise to a group of partially overlapping transition regions. It has been observed quite consistently for polymers and simpler liquids that the distribution of relaxation times for the high temperature process broadens significantly with decreasing temperature, especially near the transition region^{22,23}. Ishida^{24,25} has made the same observation in connection with the β process. Ishida's results, based on measurement of the Cole-Cole parameters, indicate that the distributions are actually broader for the β process.

It is apparent that the ability to detect a transition will depend on the magnitude of the change in the expansion coefficient or specific heat at the transition temperature. Heydemann and Guicking¹² have reported changes in the expansion coefficients for the glass and β transitions in PMMA and PVC. These are shown in Table VI.

TABLE VI

Changes in Thermal Expansion Coefficients for PMMA and PVC in Observed Dilatometric Transitions¹²

<u>Polymer</u>	<u>Change in Expansion Coefficient, Deg⁻¹ x 10⁻⁴</u>	
	<u>Glass Transition</u>	<u>β Transition</u>
PMMA	3.1	0.7
PVC	3.7	0.4

Finally, there is some evidence that in heating experiments the rate of heating has a pronounced effect on the magnitude and temperature of the observed transition. Wunderlich and Bodily¹⁸, and Martin and Muller¹⁴ have both observed a transition in polystyrene around 50°C in specific heat measurements at high heating rates. Karasz et al²⁶ failed to see this transition. All of the above investigators found behavior in some runs with the appearance of first-order transitions, i.e. sharp peaks in the specific heat in the glass transition region. Using differential thermal analysis, Wunderlich and Bodily¹⁸ have found smaller peaks at 300°K and

280°K in polystyrene. Volume experiments have also yielded anomalous results. Holt and Edwards¹⁵ noted a "contraction effect," a decrease in the coefficient of expansion in the transition region in heating experiments. Another typical result is a discontinuity in the volume in fast heating. Therefore, we propose that there are at least four factors influencing the experimental characteristics of the glass transition and lower temperature transitions:

1. The activation energy in the transition region.
2. The contribution of the relaxing mode to the expansion coefficient or specific heat.
3. The distribution of relaxation times.
4. The rate of heating.

In order to test some of the ideas expressed above, a simple dynamic model for volume relaxation has been formulated. The result has been programmed for digital computer studies.

The purpose of this study is twofold. First, we would like to determine whether or not all of the experimental features of dilatometric or specific heat amorphous transitions can be explained with the aid of a purely kinetic model. If the model succeeds here, the foundation is laid for a non-equilibrium theory for the glass transition. Secondly, if the model is successful, it can be used to extend our understanding of the glass transition.

The model is based on two assumptions. First, the over-all volume change in an isothermal volume relaxation process is the sum of contributions from all modes, i.e. vibration, group rotation, backbone rotation, translation, etc.:

$$\left(\frac{\partial v}{\partial t} \right)_{p,T} = \sum_i \left(\frac{\partial v_i}{\partial t} \right)_{p,T,V_{j+i}} \quad (15)$$

Each mode is associated with its own equilibrium expansion coefficient, α_i , which is relatively insensitive to temperature. It is known that the molar volume of organic groups and the equilibrium temperature dependences of these volumes are generally characteristic of the groups with some perturbations from the molecular environment²⁷. Therefore, we will assume that thermally induced volume changes can be represented as a linear combination of volume changes of all the contributing modes. It seems reasonable to assume that isothermal volume relaxation can be represented similarly. Thus, the contribution from the j th mode to an isothermal relaxation process can be given by

$$C_j (V - V_e) = C_j (V_0 - V_e) \exp \left[- \frac{t}{\tau_j} \right], \quad (16)$$

where

V_0 = the initial volume
 V_e = the equilibrium volume
 V = the volume at time t
 τ_j = relaxation time of the j^{th} mode
 t = elapsed time

A requirement here is that $(V_0 - V_e)$ is small enough so that τ_j is unaffected.

Kovacs²⁸ and Hirai and Eyring²⁹ have used expressions of this form in the study of isothermal volume relaxation in quenched polymers and viscous liquids.

If equation (16) is summed over all modes, we obtain

$$V - V_e = (V_0 - V_e) \sum_i C_i \exp \left[\frac{-t}{\tau_i} \right] \quad (17)$$

where $\sum_i C_i$ is taken as unity. Thus, we have the result that the over-all volume relaxation can be given as a linear combination of relaxations of individual modes.

Here we shall be concerned only with thermally induced departures from the equilibrium volume, and so the coefficient C_j assumes a value of α_j / α_T . Here α_j is the expansion coefficient for the j^{th} mode and α_T is the over-all thermal expansion coefficient, $\sum_i \alpha_i$.

In this instance we wish to use the model to simulate only one transition at a time. It is reasonable then to consider a system with two relaxation times, a long one, τ_A , associated with the transition, and a short one, τ_B , which actually represents all of the shorter relaxation times of the system. The assumption is made here that $\tau_A \gg \tau_B$ in the temperature range of interest.

The tacit assumption is also made that any relaxation times longer than τ_A are so large that there are effectively no contributions from these modes to the volume relaxation of the system, and α_T contains no contributions from these modes. The assumption of two relaxation processes, one effectively instantaneous and one with an intermediate relaxation time, is not new. Alfrey, Goldfinger, and Mark³⁰ suggested this in 1943, and Spencer and Boyer³¹ and later Spencer³² made the same assumption in treating volume relaxation in polymers.

Equation (17) can now be reduced to

$$V - V_e = (V_o - \Delta V_B - V_e) \exp \left(- \frac{t}{\tau_A} \right), \quad (18)$$

where

$$\Delta V_B = \frac{\alpha_B}{\alpha_A + \alpha_B} (V_o - V_e). \quad (19)$$

Thus, all low temperature processes are treated as a single instantaneous relaxation mode. ΔV_B is equivalent to the instantaneous relaxation observed in mechanical measurements.

Unfortunately, Equation (18) cannot be used directly to simulate a dilatometry experiment with a fixed rate of temperature change. It is possible to simulate such an experiment, however, with a series of closely spaced isothermal relaxations, each with the form of a temperature step following by relaxation during a time step. As the step size approaches zero, this process will approach the continuous process. The steps can be varied until convergence is indicated. In order to use this method, we first put Equation (18) into the form

$$V = V_e + (V_o - V_e) \frac{\alpha_A}{\alpha_A + \alpha_B} \exp \left[- \frac{t}{\tau_A} \right] \quad (20)$$

By using this approach, we circumvent the problem of nonlinearity faced by Kovacs³³. In his work, the sample is quenched from an elevated temperature to some temperature in the transition region and volume relaxation is observed after thermal equilibrium is attained. The volume dependence of the bulk retardation time becomes significant in such experiments, and must be accounted for.

It is well known that the relaxation time obeys the WLF equation or Fulcher equation above the glass temperature but deviates sharply in and below the transition region. It has been reported by Sommer³⁴ that the mechanical relaxation time for PVC approaches a limiting value below the glass temperature.

Fox and Flory³⁵ predicted that the melt viscosity of polystyrene would approach a constant value below T_g based on free-volume considerations. This phenomenon has been observed experimentally in studies of the viscosity and relaxation time of inorganic glasses^{36,37}. The reason for this is presumably the non-equilibrium nature of the glassy state. In order to describe this behavior below the transition, it was necessary to go back to the model. Equation (17) indicates that at some temperature below the A transition T_A becomes very large and the volume contribution associated with the Ath mode is effectively constant. This suggests that the relaxation time T_A is determined solely by the volume contribution of the Ath mode in and below the transition region. The apparent temperature is then the temperature at which the present volume would be the equilibrium volume. We have, after taking out the contribution from short relaxation times,

$$\frac{\Delta T_{app}}{\Delta T_{act}} = \frac{\text{Observed contraction due to Ath mode}}{\text{Equilibrium contraction due to Ath mode}}, \quad (21)$$

which reduces to

$$T_{app} = T_{ref} - \frac{[V_{ref} - V_{act} - \alpha_B (T_{ref} - T_{act})]}{\alpha_A}. \quad (22)$$

The terms are

- T_{app} = the apparent temperature of the Ath mode
- T_{ref} = an arbitrary reference temperature where equilibrium behavior of the Ath mode is observed
- V_{ref} = the equilibrium volume at T_{ref}
- T_{act} = the actual temperature
- V_{act} = the volume at T_{act} .

Note that α_A and α_B are in the form $(\partial V / \partial T)_p$ in Equation (22).

This model deviates somewhat from the "fictive temperature" approach of Tool³⁸ and Ritland³⁹. In Tool's formulation, the relaxation rate of the system is determined by both the fictive temperature (corresponding to the apparent temperature) and the actual temperature, while in this formulation the apparent temperature alone determines the relaxation time. It has been found that the activation energy for

viscous flow at constant volume is generally large⁴⁰, indicating a strong dependence on the actual temperature, but this is only known for liquids well above their glass temperature. The glassy state is quite different from the normal liquid state, and it is quite conceivable that transport properties will exhibit volume and temperature dependence unlike that of low viscosity liquids.

A comparison of the results of Sommer³⁴ and Saito³⁵ for PVC indicated the equivalence of dielectric and mechanical relaxation times for this polymer. Therefore, it was decided to use dielectric data for the high temperature dispersion in PVC to obtain a value for τ_A in Equation (20). Saito's data had already been fitted⁵ with an expression of the form

$$\log \tau = \log A/T + \frac{B}{T-T_0}, \quad (23)$$

based on the Fulcher¹¹ equation:

$$\log \eta = A + \frac{B}{T-T_0}. \quad (24)$$

The Fulcher equation has been shown to be very accurate when applied to simple liquids and polymers, where the activation energy is nearly constant at high temperatures and increases rapidly in the region above the glass temperature. T_0 is the temperature at which the extrapolated viscosity and activation energy go to infinity, and, as one might expect, is experimentally unattainable. Equation (23) uses the general form of the Fulcher equation to describe the behavior of the average relaxation time of a particular mode of the system and yields the free energy of activation.

In the actual computation, the apparent temperature (T_{app}) is first determined after taking each time-temperature step using Equation (22). This value for T_{app} is then used in Equation (23) in place of T in the calculation of the relaxation time. Until the transition region is entered, T and T_{app} are identical. In and below the transition region, the system is in a non-equilibrium state and T_{app} is always greater than T . In some of our computations, we have used equilibrium relaxation times all the way in order to demonstrate the difference between the equilibrium and non-equilibrium treatments. In these cases, Equation (23) is used as it stands, with the actual temperature rather than T_{app} .

We also decided to consider volume relaxation for both the α and β processes in PMMA and the α processes in poly(methyl methacrylate) and poly(vinyl acetate). The necessary dielectric relaxation data was taken from earlier analyses of Saito's results⁵. A simple Arrhenius temperature dependence was found to be quite satisfactory for the β process in PMMA.

In addition, we decided to simulate one experiment using extrapolated equilibrium relaxation times all the way down through the transition region. This was done for the α process in poly(vinyl acetate).

The problem was programmed in the Fortran II computer language, and the program was run on a Scientific Data Systems 925 Computer in the Mathematical Analysis Section.

Results

Thus far, cooling experiments have been simulated for the three processes described above, with cooling rates ranging from 0.36 degrees per hour to 36,000 degrees per hour. Expansion coefficients above and below the transitions were taken from Heydemann and Guicking¹².

Figures 6 through 11 give the computed volume-temperature curves. The transition temperatures have been obtained in the usual way, i.e. as the intersections of the extrapolated volume lines above and below the transition region. The glass transition for PVC over four decades of cooling rates ranged from 345°K to 354°K. Heydemann and Guicking¹² report values of 345°K at 7 degrees per hour and 348°K at 25 degrees per hour. The computed values at 3.6 and 36 degrees per hour, 347°K and 349°K, respectively, are essentially identical to these. The computed glass temperatures for PMMA ranged from 372°K to 382°K. Literature values for commercial free-radical PMMA generally fall in this region. For example, Martin et al⁴¹ reported a transition at 373°K, Holt and Edwards¹⁵ found one at 372°K with a heating rate of 60 degrees per hour, and Heydemann and Guicking¹² observed a transition at 375°K with a 25 degree per hour cooling rate. The computed value of 374°K with a cooling rate of 36 degrees per hour agrees very well with these observations.

The computed β transition temperature in PMMA ranged from 215°K to 242°K over three decades of cooling rates. This great variation in temperature can be attributed to the small activation energy for the β process, ~ 19 kcal.^{16,20} As Figure 8 shows, the transition region is very broad, with curvature existing in the volume-temperature plot 50 degrees below the transition temperature. This may account for the discrepancy between the computed transition temperatures and the values of 266°K and 296°K obtained by Heydemann and Guicking¹² and Holt and Edwards¹⁵, respectively. However, we feel that the problem here is one of picking straight lines. Martin, Rogers and Mandelkern⁴¹ found that the volume-temperature behavior of PMMA below T_g could be represented either

Figure 6

Computed Volume-Temperature Curves for PVC Showing Glass Transition

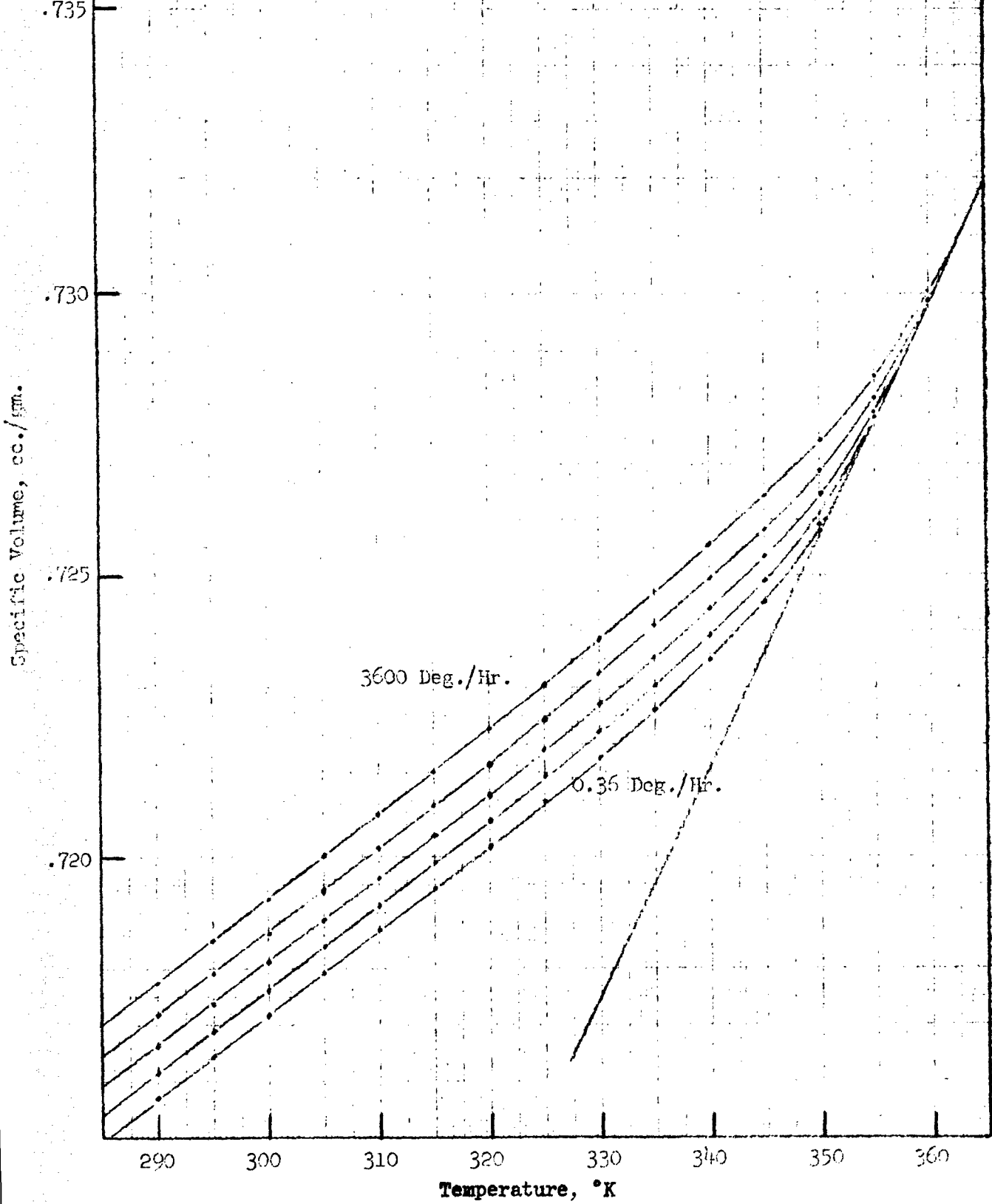


Figure 7

Computed Volume-Temperature Curves for PMA Showing Glass Transition

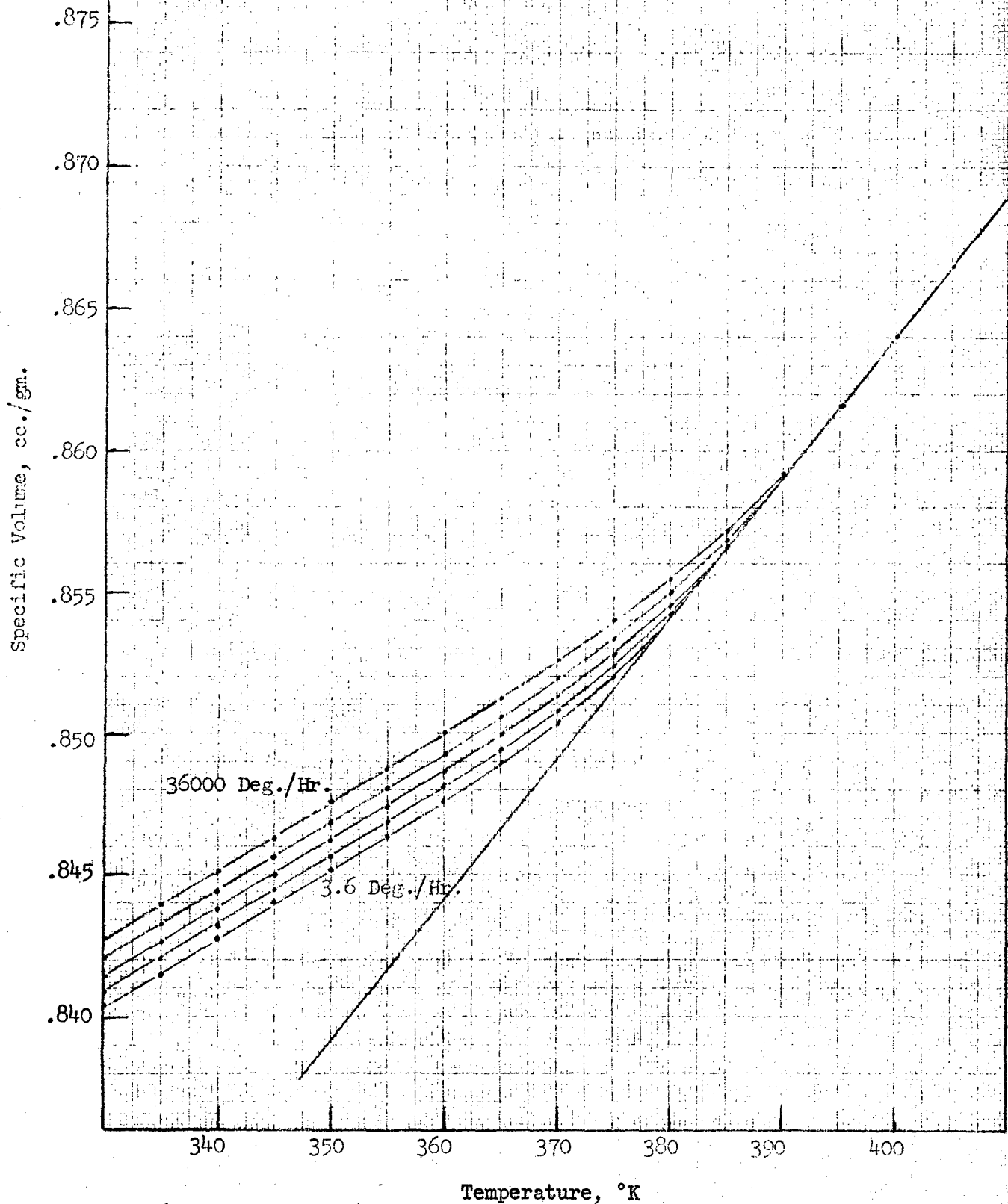
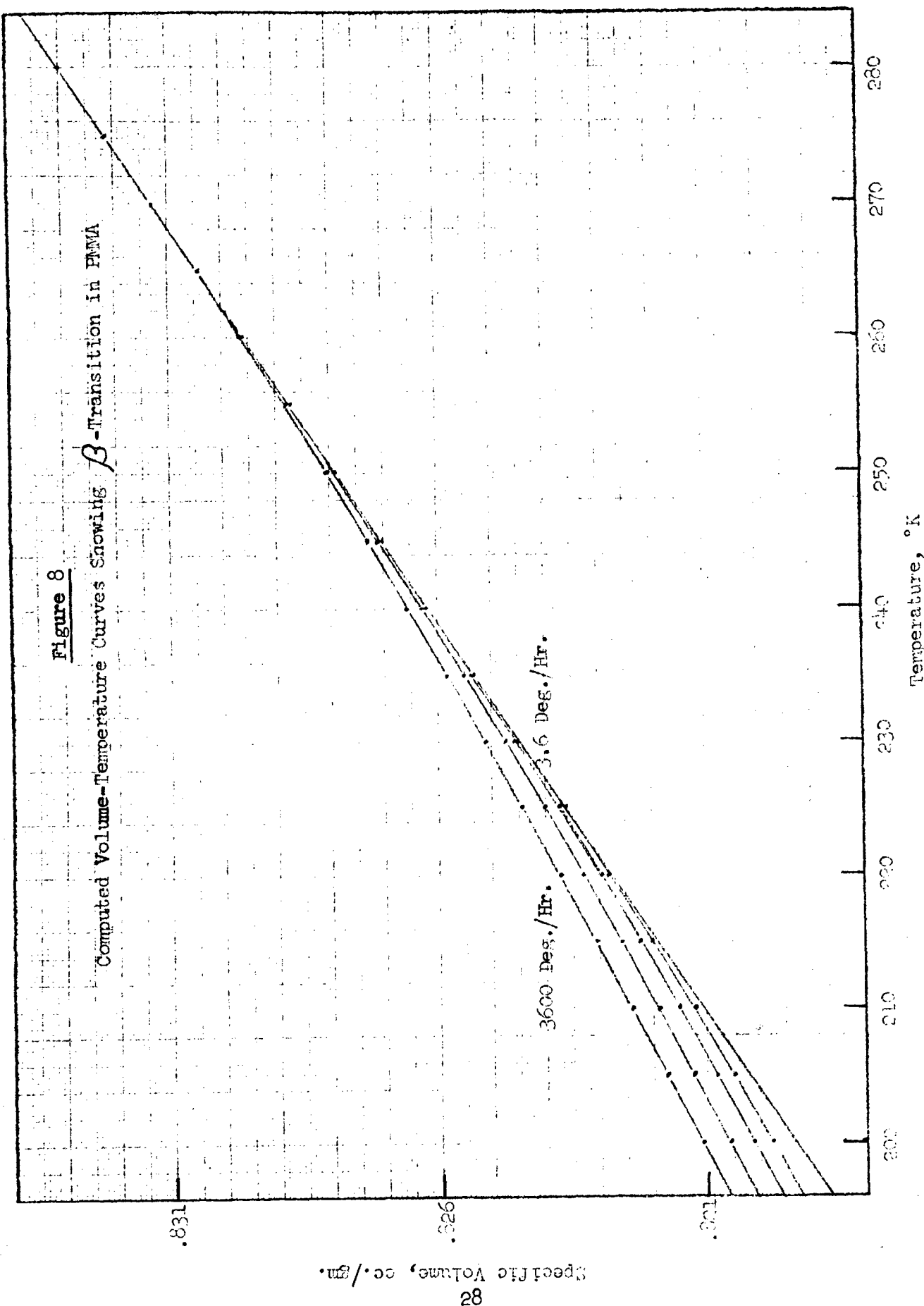


Figure 8

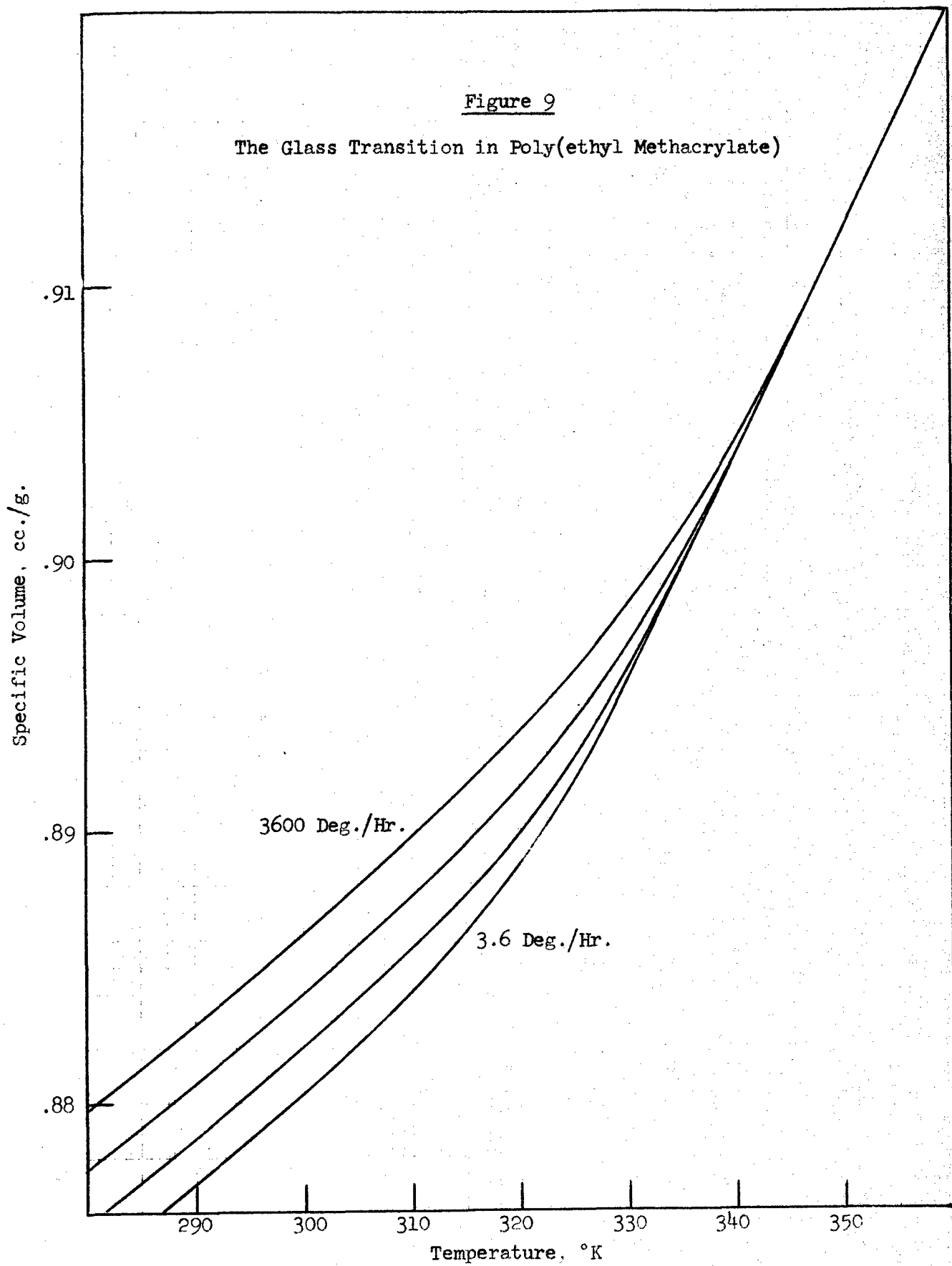
Computed Volume-Temperature Curves Showing β -Transition in PMMA



Specific Volume, cc./gm.

Figure 9

The Glass Transition in Poly(ethyl Methacrylate)



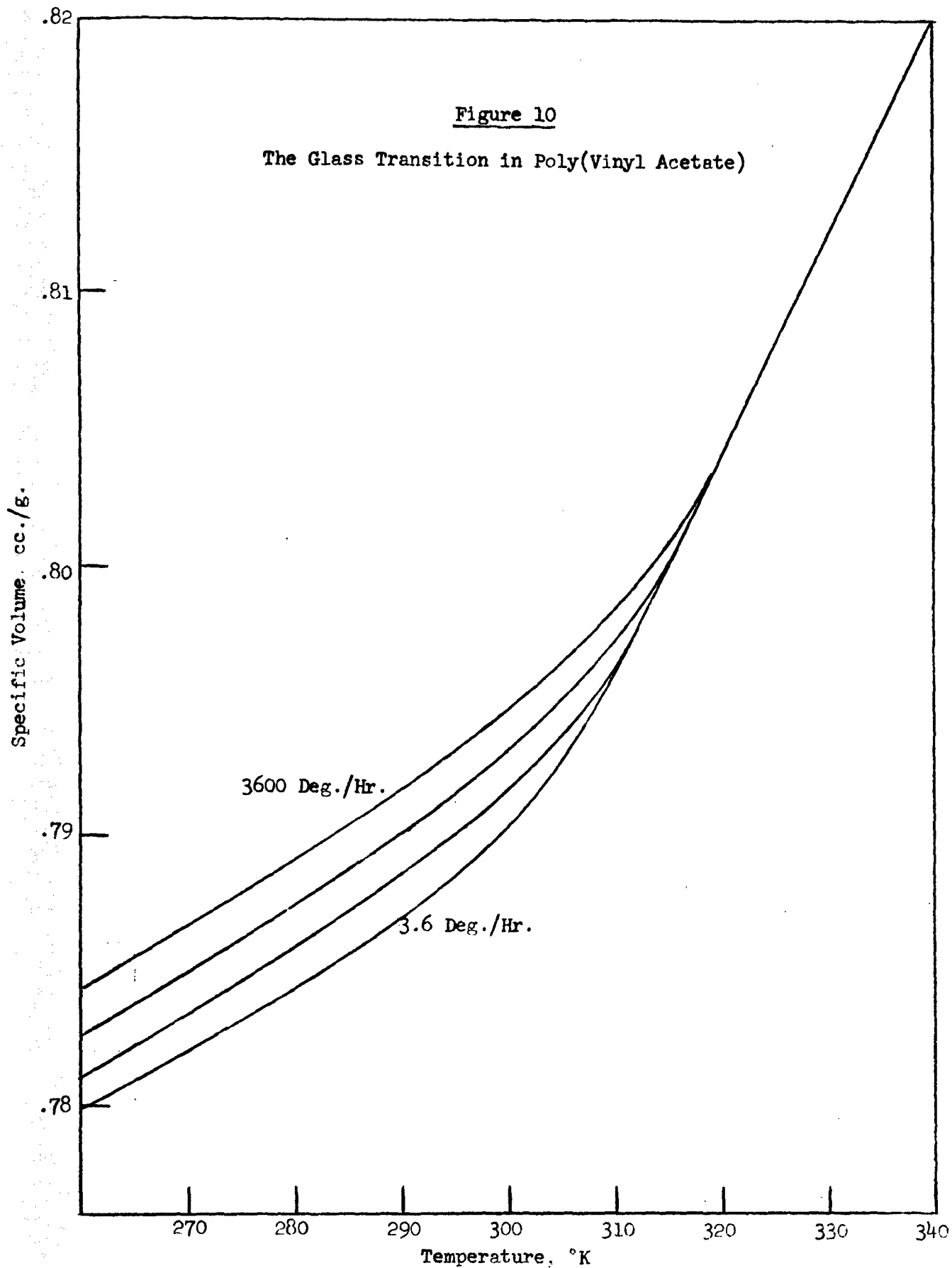
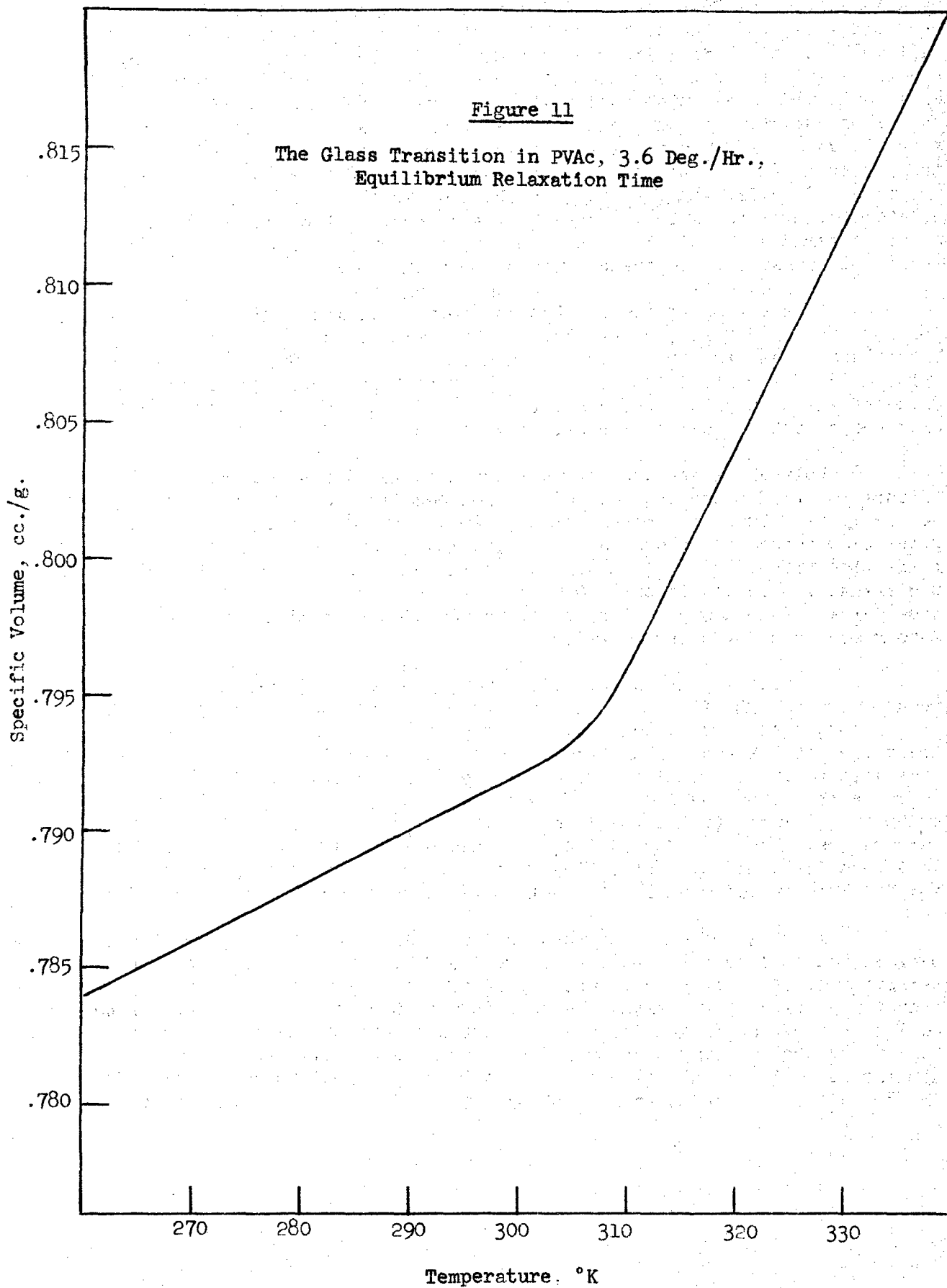


Figure 11

The Glass Transition in PVAc, 3.6 Deg./Hr.,
Equilibrium Relaxation Time



by a gradual curve or a series of intersecting straight lines. Heydemann and Guicking¹² reported a weak 335°K dilatometric transition in PMMA. We believe that this transition may be associated with the motion of isotactic sequences in the backbone. Now, the nonequilibrium nature of the motion of a particular mode in and below its transition region gives rise to a degree of curvature in the volume-temperature curve which persists for some distance below the transition temperature. Combine this factor with the presence of transitions at 375°K, 335°K, and 280°K, and one can see why it would be difficult to resolve the individual transitions dilatometrically below T_g . Further, if a tangent to the volume-temperature curve is selected just below the onset of the transition region, the indicated transition temperature would approach 270°K.

Figure 9 shows the results for poly(ethyl methacrylate). A cooling rate of 3.6 degrees per hour gives a transition at 320°K (47°C). Literature values for this polymer are around 65°C, but Saito¹⁶ reports a value of 50°C for his polymer. It may be that Saito's polymer contained diluents which depressed the glass temperature. At any rate, the agreement with the computed results is remarkable.

Poly(vinyl acetate) gives a computed glass temperature of 303°K (Figure 10) with a cooling rate of 3.6 degrees per hour. This value agrees perfectly with the one reported by Saito¹⁶ and the accepted value. The glass temperature for the same polymer, computed with equilibrium relaxation times, is 307°K (34°C), as shown in Figure 11. The width of the transition region is only 10 degrees in the equilibrium relaxation time curve. The incorporation of volume dependence broadens this to a more reasonable 25-30 degree width.

Figures 12, 13, and 14 illustrate the rate dependence of the two transitions in PMMA and the transition in PVC. The upward curvature seen in all three cases is caused by the existence of a lower limit for each transition at the temperature where the extrapolated equilibrium relaxation time goes to infinity. This aspect of the dilatometric transitions supports the Gibbs and DiMarzio⁴² theory, which predicts an equilibrium transition temperature as the lower limit of the glass transition temperature. The rate dependence of T_g has been plotted linearly for PMMA in Figure 15, exhibiting essentially the same behavior seen by Wunderlich and Bodily¹⁸ in differential thermal analysis measurements on polystyrene.

A matter of some interest is the determination of the relationship between the cooling rate and the relaxation time at the transition temperature. As Figure 16 shows, a plot of the logarithm of τ at the transition temperature versus the logarithm of the cooling rate appears to be linear for the α transitions (T_g), but shows negative deviations in $\log \tau$ for the β transition at low cooling rates. This deviation appears to be the result of picking a tangent too close to the upper end of the transition region at small cooling rates, as can be seen in Figure 8.

Figure 12

The Variation of T_g with Cooling Rate, PVC

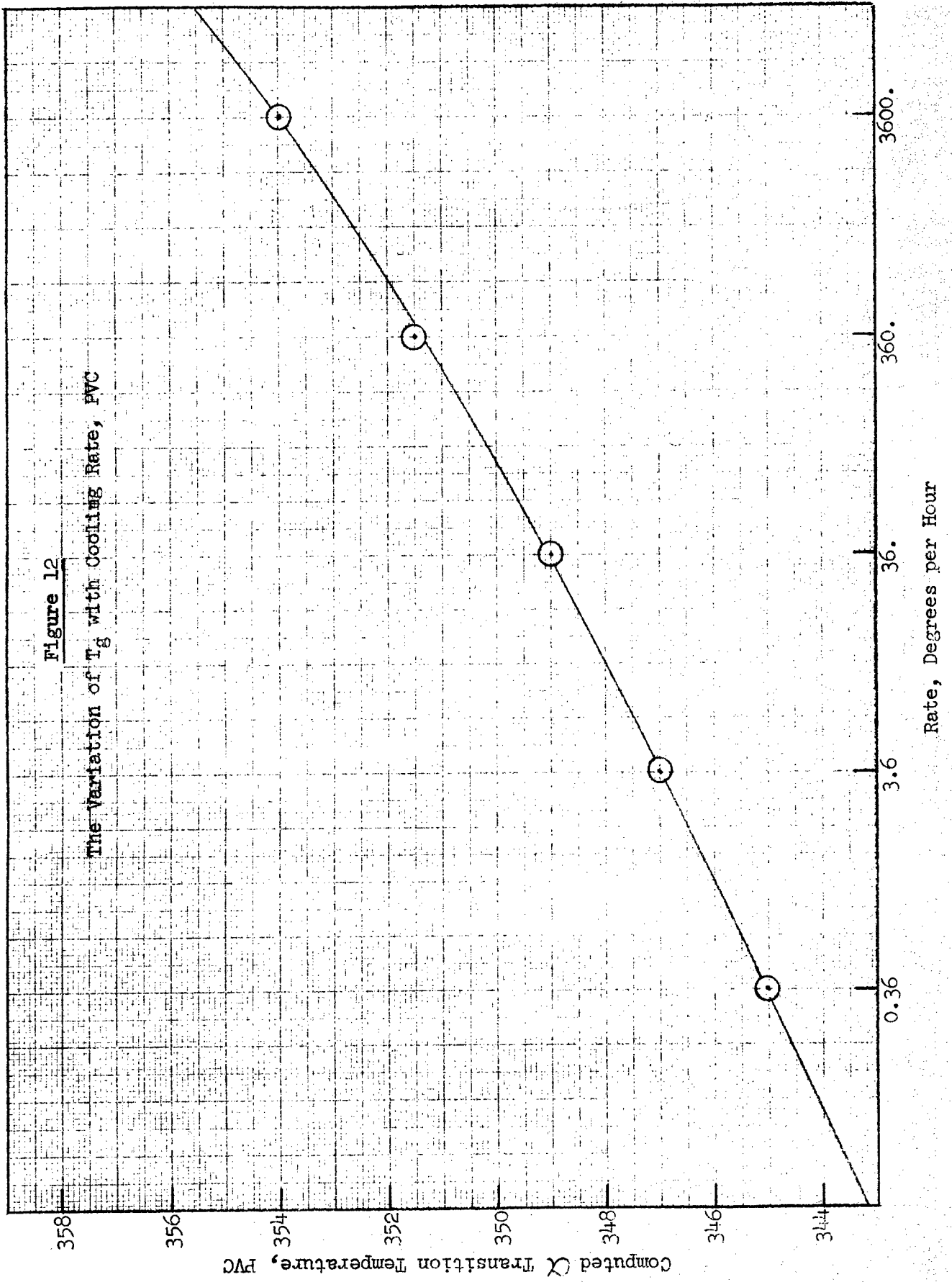


Figure 13

The Variation of T_g with Cooling Rate, PMMA

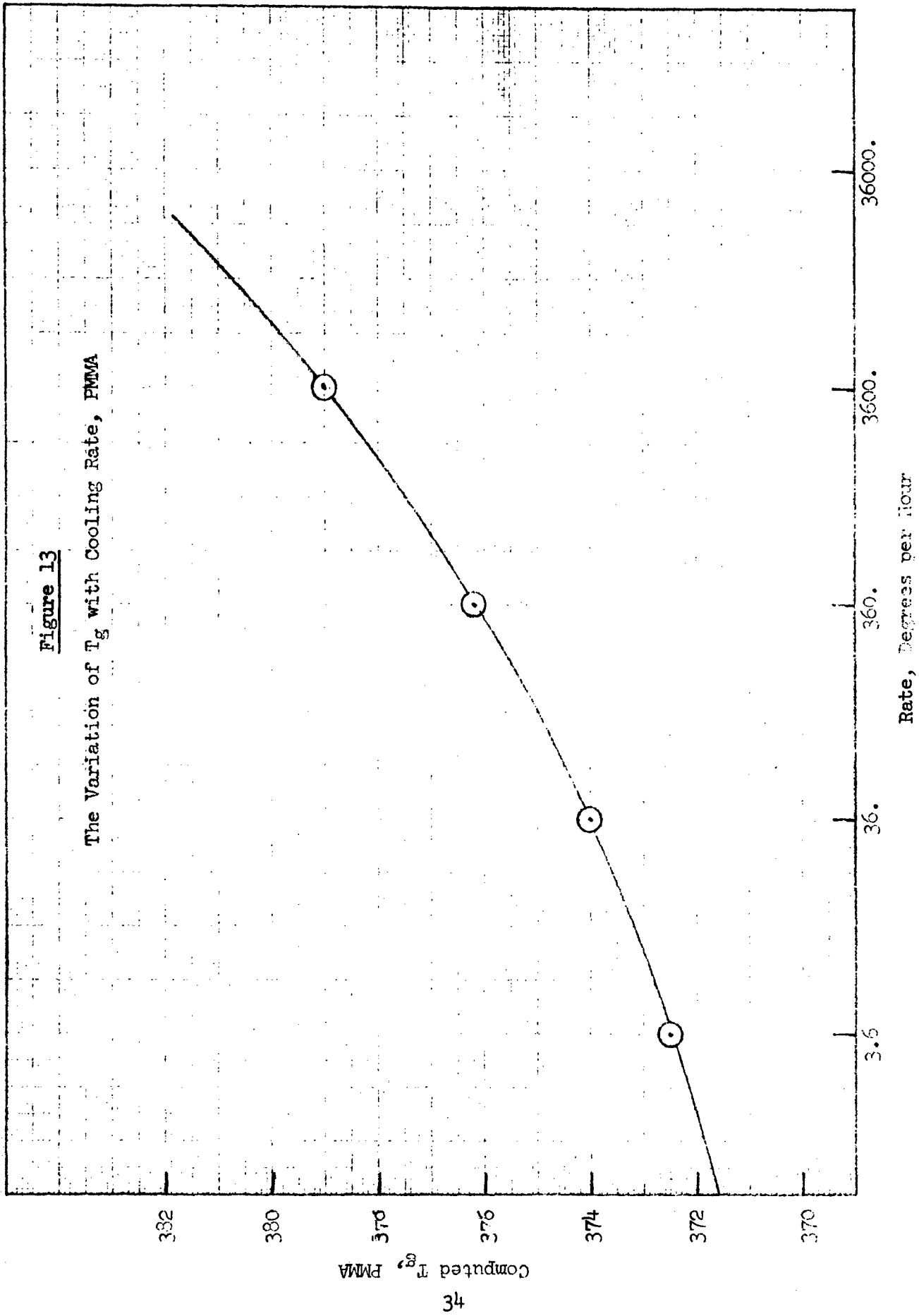


Figure 14

The Rate-Dependence of the β Transition in PMMA

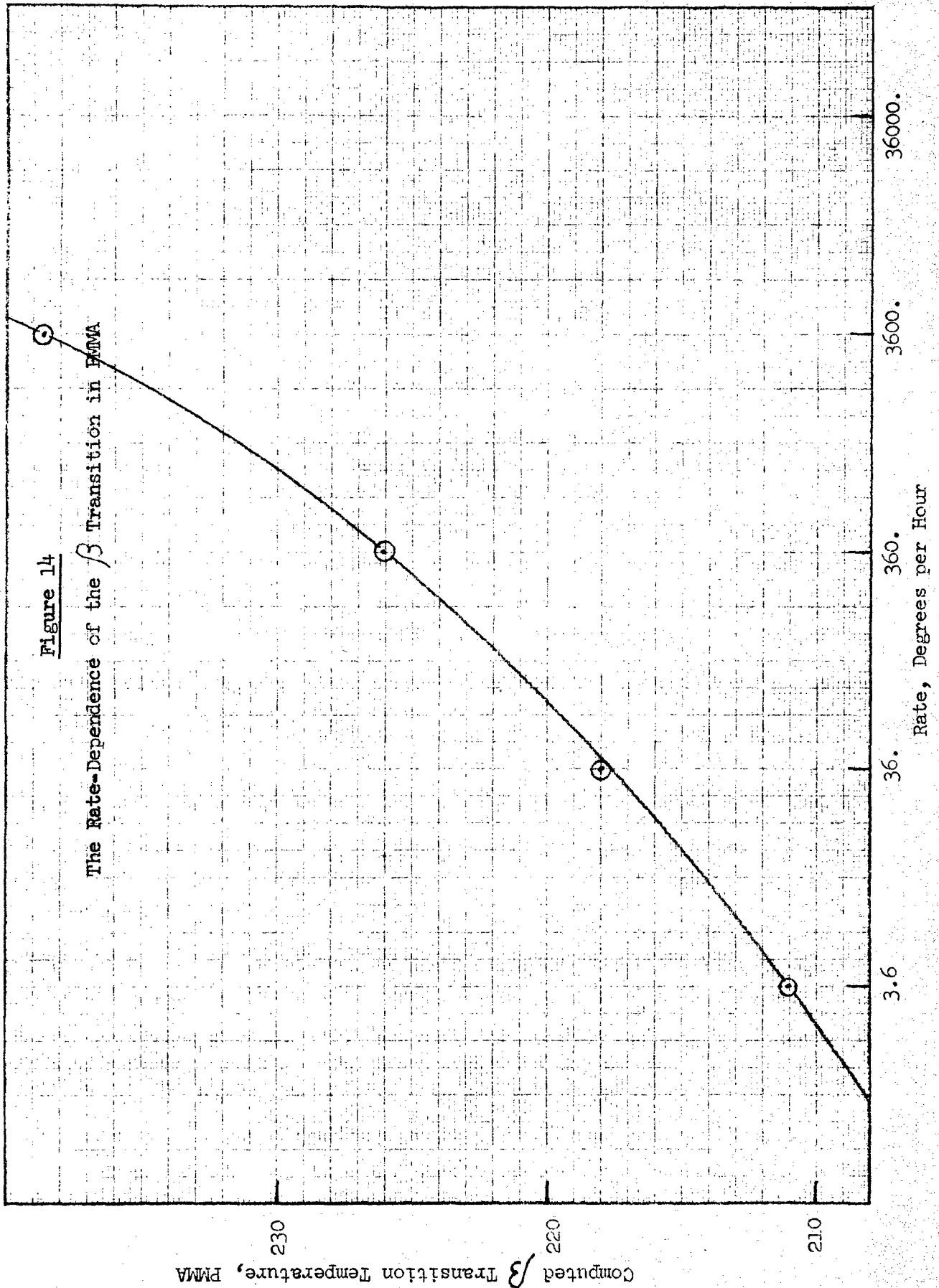


Figure 15

Linear Plot of the Variation of T_g with Cooling Rate, PMMA

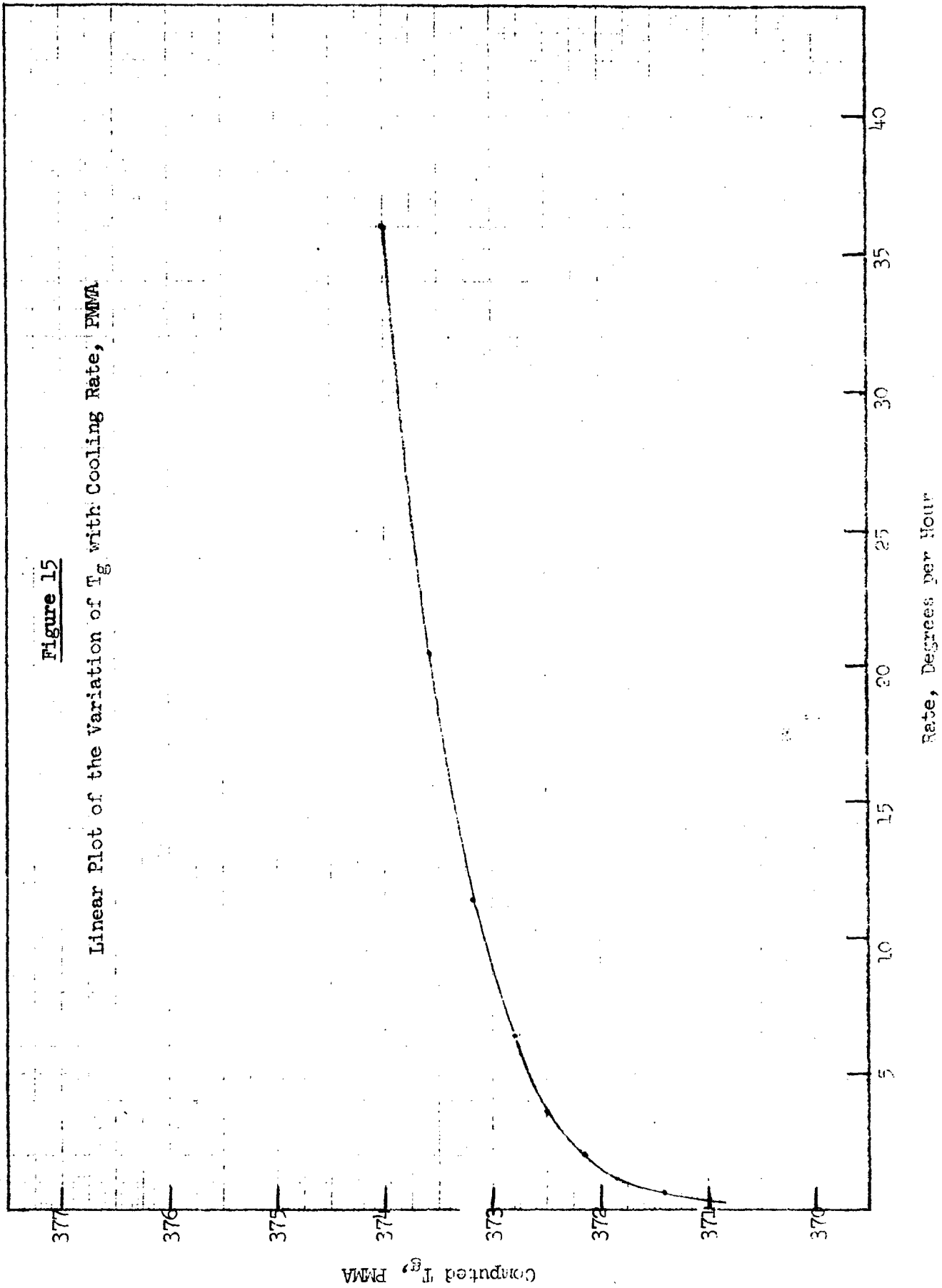
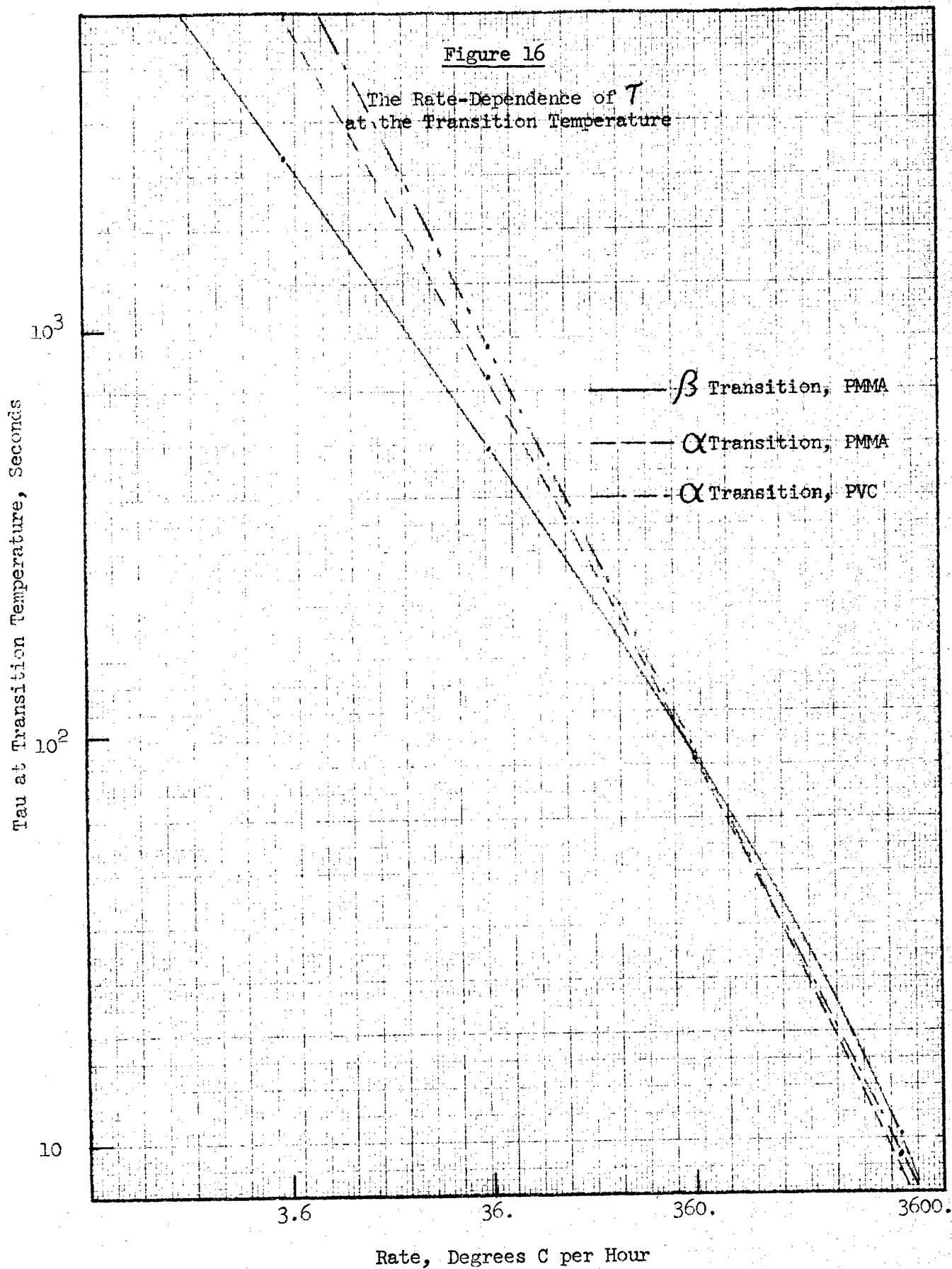


Figure 16

The Rate-Dependence of T
at the Transition Temperature



The result is the selection of a value of T_g which is too high, giving a small value for τ at the apparent transition temperature. This, of course, is just the sort of error we discussed above. It has been found then that, as we might expect, a plot of $\log \tau$ versus \log (rate) is linear with a slope of -1. The value of τ at the transition temperature is about as expected, approximately 17 minutes at 36 degrees per hour.

Finally, we have computed the values of the relaxation times passing through the transition region at different cooling rates for each of the transitions studied. The relaxation time has been assumed as a first approximation to be a function of volume only in and below the transition region as already described. The results are given in Figures 17, 18, and 19. Sommers'³⁴ results for PVC are shown for comparison in Figure 17, indicating reasonable agreement with the simple volume-model. It should be mentioned here that this model was selected empirically in order to approximate experimentally observed behavior. There is certainly a good deal of support for such a model among the various free-volume theories of molecular motion^{1,2,43}, but we would prefer not to be drawn into the controversy on free volume at this point.

It was mentioned in this report that several investigators have observed unusual volume and specific heat effects in studies of amorphous transitions when heating rather than cooling was used. These effects apparently result when samples which have been cooled at one rate or have simply been stored are then heated at some other rate, giving rise either to early approaches to equilibrium (low heating rates) or to delayed approaches (high rates), which have the appearance of contractions or first-order transitions, respectively. Such phenomena can be explained qualitatively assuming either equilibrium or nonequilibrium relaxation times in the transition region. However, it should be possible to obtain additional evidence for nonequilibrium relaxation times as proposed here by quantitative comparisons with experimental results. These effects in any case will be more pronounced where large activation energies and large changes in expansion coefficients are involved, at high heating rates. This explains why the β transition in polystyrene has been observed at high heating rates by Wunderlich¹⁸ but not seen at low rates²⁶.

Conclusions

It has been shown with the aid of a simple volume-relaxation model that the ability to resolve dilatometric transitions in amorphous polymers is affected by at least three factors: the change in the coefficient of expansion accompanying the transition, the rate of heating, and the activation energy in the transition region. In addition, it is reasonable to assume that a broad distribution of relaxation times will broaden the transition region.

The dilatometric glass transition temperatures of PVC, PMMA, PVAC, and PEMA have been computed accurately with the assumption that the dielectric relaxation time is equal to the volume relaxation time in

Figure 17

Computed Relaxation Time (α Process)
for PVC at Different Cooling Rates

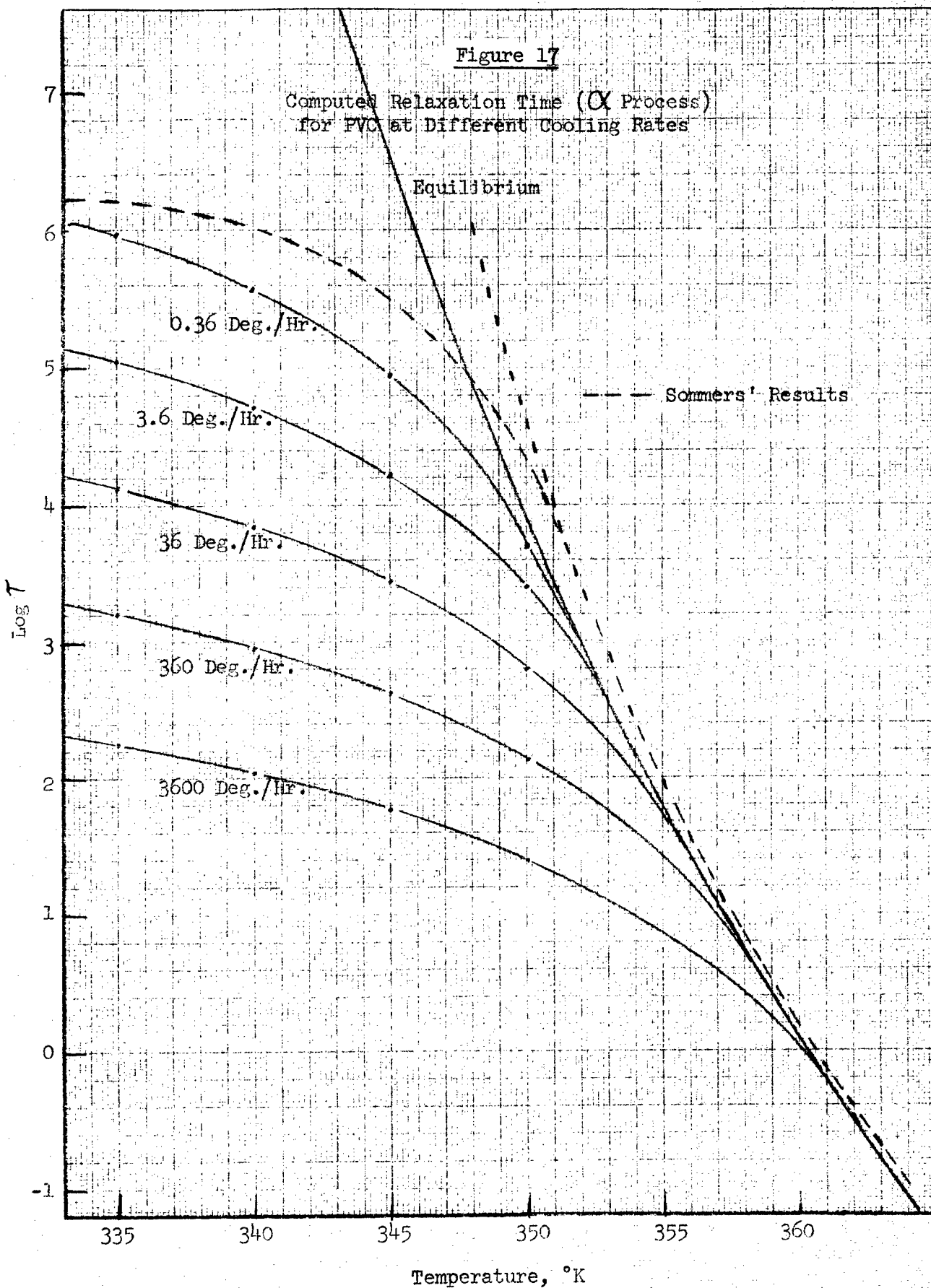
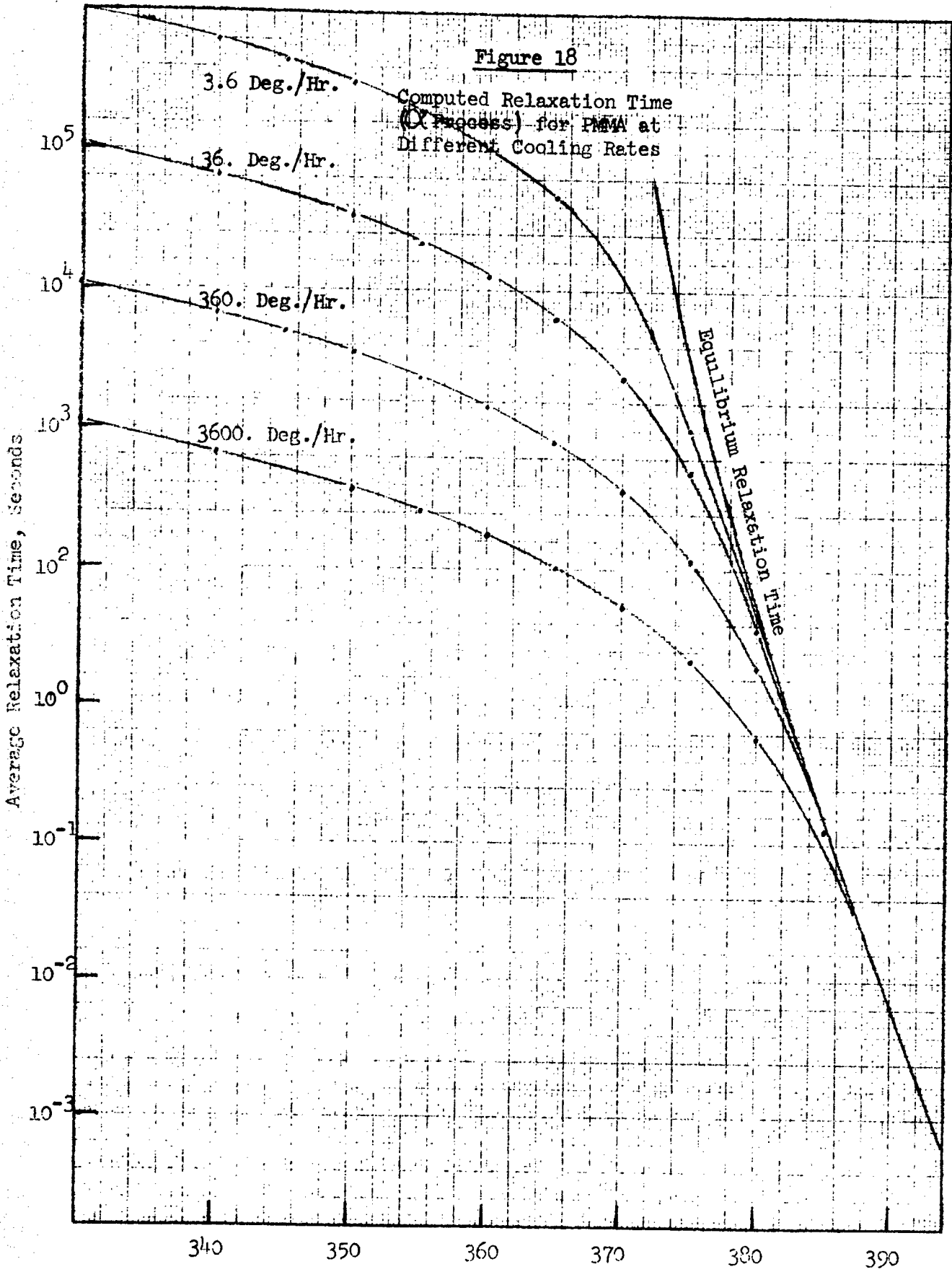


Figure 18

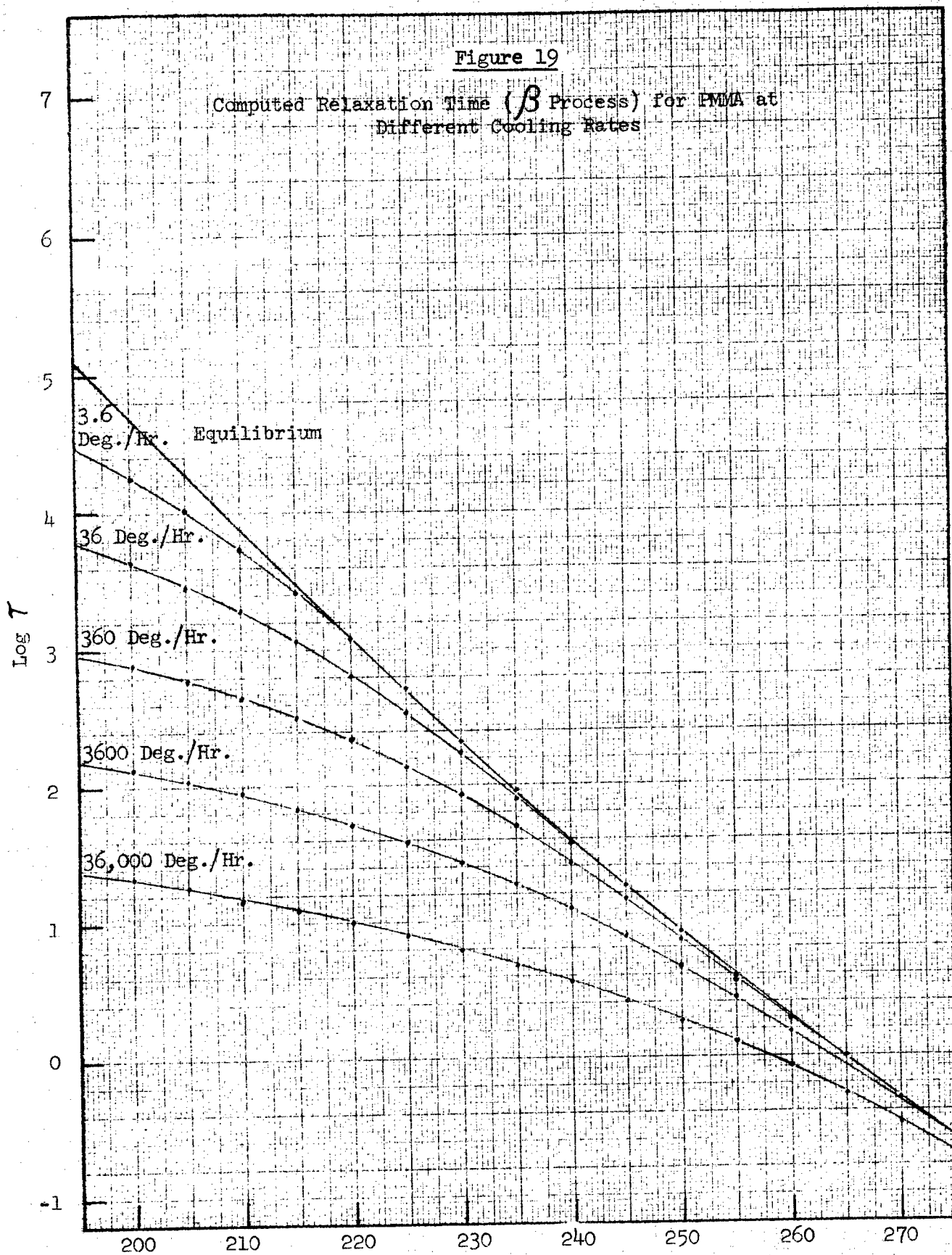
Computed Relaxation Time
(Process) for PMA at
Different Cooling Rates



Temperature, °K

Figure 19

Computed Relaxation Time (β Process) for PMMA at
Different Cooling Rates



Temperature, °K

the temperature region above the transition temperature. Our success here indicates that this assumption is reasonable. It is still possible that the two relaxation times could differ slightly, since this would mean a small difference in the observed glass temperature. This could prove to be important in developing a glass-transition theory based on relaxation times.

Although the experimental glass temperature is determined by dynamic considerations, it appears that there is a lower limit to the glass temperature. As the cooling rate approaches zero, T_g must approach a temperature corresponding to the T_0 in the Fulcher equation¹¹. This is in basic agreement with the Gibbs and DiMarzio⁴² theory, which predicts an equilibrium second-order transition temperature T_2 as a lower limit to T_g . This suggests that a reasonable glass temperature theory might start first by predicting a value for T_2 based on equilibrium statistical mechanics, and then use this result as a stepping stone to a nonequilibrium approach. Adam and Gibbs⁴ have formulated a kinetic theory for relaxation in glass-forming liquids along these lines, for the theory requires a value for T_2 .

3. Gibbs-DiMarzio Theory of the Glass Transition

A. Introduction

Statistical-mechanical calculations of the properties of liquids composed of long chain molecules, based on the Flory-Huggins lattice model, indicate that crystallization of polymers⁴⁴, and the formation of glasses^{42,45} can be related to a fundamental measure of chain stiffness, the "flex energy." In the rotational-isomeric model of a molecular chain, the flex energy represents the average energy required to rotate one of the chain bonds from its lowest-energy conformational state to one of higher energy. Changes in chain conformation make an intramolecular contribution to the system energy, proportional to the number of bonds in higher energy states. The total energy of the system in any given state is the sum of the individual energies of the molecules plus the intermolecular energy. In the Gibbs-DiMarzio^{42,45} theory, the intermolecular energy is calculated by means of a nearest-neighbor approximation in which it is assumed that the energy required to create a "hole," or vacant lattice site, is proportional to the number of "van der Waals bonds" between molecules which must be broken.

Gibbs and DiMarzio evaluated the configurational entropy, or entropy difference between the randomly disordered state and a hypothetical state of perfect order, on the basis of the above considerations. They found that the configurational entropy vanishes at a temperature above absolute zero, and proposed that this temperature, T_2 , is the lower limit to the glass temperature as the time scale of the experiment approaches infinity.

The Gibbs-DiMarzio theory accounts satisfactorily for the effects of molecular weight⁴², copolymer composition⁴⁶, and diluents⁴⁷ on polymer glass temperatures. However, no satisfactory method has heretofore been developed for predicting the flex energy and intermolecular energy, from which the glass temperature could be calculated.

B. Flex Energy in n-Alkanes

Application of the Gibbs-DiMarzio theory to transition temperatures for n-alkanes⁴⁸, calculated from viscosity data, resulted in an estimated 490.8 cal./mole flex energy for a polymethylene chain, in agreement with determinations by other methods. For this comparison with experimental results, the relations given in Reference 42 were used. However, a long chain approximation had been made in deriving those relations, and it was of interest to see if a better fit to the data on the lower members of the n-alkane series could be achieved with the exact relation. At the same time, it was felt desirable to include the intermolecular energy contribution to the configurational entropy, which had been neglected in the original study^{5,48}, since this can be done without difficulty.

The exact expression for the configurational entropy, S_1 , of a system composed of n_x chains of x backbone units packed on a lattice of coordination number z is given by Equation (14) of Reference 45:

$$\begin{aligned}
 S_1/Rxn_x = & \frac{z-2}{2} \ln \left(\frac{V_o}{S_o} \right) + \frac{n_o}{xn_x} \ln (V_o^{z/2-1}/S_o^{z/2}) \\
 & + x^{-1} \ln \frac{[(z-2)x + 2](z-1)}{2} + x^{-1} \ln \sum_i \exp (-E_i/RT) \\
 & + \frac{\sum_i (E_i/RT) \exp (-E_i/RT)}{x \sum_i \exp (-E_i/RT)} . \quad (25)
 \end{aligned}$$

R is the gas constant, V_o the fractional free volume, n_o the number of unoccupied sites and E_i the intramolecular energy of a molecule in the i th conformation. The following relationships can also be found in Reference 45:

$$V_o = n_o/(xn_x + n_o) , \quad (26)$$

$$S_o = 1 - S_x , \quad (27)$$

$$S_x = \frac{[(z-2)x + 2]n_x}{[(z-2)x + 2]n_x + zn_o} , \quad (28)$$

$$\ln (V_o^{z/2-1}/S_o^{z/2}) = \alpha z S_x^2 / 2RT , \text{ and} \quad (29)$$

$$\sum_i \exp (-E_i/RT) = \frac{1}{2} \sum_{k=1}^m \exp (-\epsilon_k/RT)^{x-3} . \quad (30)$$

α is the interaction energy between occupied nearest-neighbor lattice sites, relative to the energy when one of the sites is vacant. The

summation on the right hand side of Equation (30) is made over the m conformational isomers of energy ϵ_k available to each chain bond. If there are $m-1$ conformers of energy ϵ relative to the single preferred conformer, then

$$\sum_i \exp(-E_i/RT) = \frac{1}{2} [1 + (m-1) \exp(-\epsilon/RT)]^{x-3}. \quad (31)$$

The last term in Equation (25) is simply the average value of E/xRT , which can be written in terms of the flex energy as follows:

$$\bar{E}/xRT = \frac{(x-3)(\epsilon/xRT) \exp(-\epsilon/RT)}{1 + (m-1) \exp(-\epsilon/RT)}. \quad (32)$$

Making the appropriate substitution in Equation (25), we obtain

$$\begin{aligned} S_1/Rxn_x &= \frac{z-2}{2} \ln \left[1 - \frac{2(1-V_0)}{z} + \frac{2(1-V_0)}{zx} \right] + \frac{V_0 \alpha z}{(1-V_0)2RT} \\ &\left\{ 1 + \frac{zxV_0}{[(z-2)x + 2](1-V_0)} \right\}^{-2} + x^{-1} \ln \left\{ [z-2]x + 2 \right\} / 2 \left\{ + x^{-1} \ln \frac{1}{2} \right. \\ &+ \frac{x-3}{x} \left\{ \ln [1 + (m-1) \exp(-\epsilon/RT)] \right. \\ &\left. \left. + \frac{\epsilon/RT \exp(-\epsilon/RT)}{1 + (m-1) \exp(-\epsilon/RT)} \right\} \right\}. \quad (33) \end{aligned}$$

If z , V_0 , α , m and ϵ are known, Equation (33) can be solved for the second-order transition temperature, T_2 , as a function of x by setting $S_1 = 0$.

The pair potential α can be estimated from the heat of vaporization by the relation

$$\alpha z/2 = E_v/x \quad (34)$$

where E_v is the energy of vaporization of the ideal gas. At 25°C, E_v increases by about 1080 cal. mole⁻¹ per methylene unit in the n-alkanes. This value is used for the quantity E_v/x .

As described in the Summary Technical Report of July, 1965⁵, the best empirical equation found for representing the viscosity-temperature data on n-alkanes was a modified Fulcher equation:

$$\log (\eta/d) = \log (A/T) + B/(T-T_0) , \quad (35)$$

where A, B and T_0 are adjustable parameters. The best-fit values of T_0 for each compound were shown in Table IV, page 8 of that report and are plotted in Figure 20 of this report as a function of the number of carbon atoms, x. A non-linear least squares estimation procedure was used to determine that value of ϵ which gives the best agreement between T_2 , calculated from Equation (33), and the observed values of T_0 , for all the n-alkanes from hexane to eicosane. The parameters z and V_0 were varied over a reasonable range, and while all the possibilities were not exhausted, a very satisfactory fit was found for the case of z = 6, $V_0 = 0.04$ and $\epsilon = 340.0$ cal. mole⁻¹. There are, of course, m = 3 rotational isomers for each chain bond in a n-alkane. The calculated transition temperatures are shown as the curve in Figure 20.

In the earlier attempt^{5,48} to use the Gibbs-DiMarzio theory on n-alkane data, it was found that negative values of T_0 were predicted for $x \leq 5$. This resulted from the use of the approximate relations in Reference 42. As is evident from Figure 20, Equation (33) makes a reasonable prediction for all the n-alkanes, with a reasonable value for the flex energy. The errors for methane and ethane are not surprising, in view of the fact that this is a theory for polymers. The observed value of T_0 for butane is out of line with the others, and this deviation is not predicted by the theory.

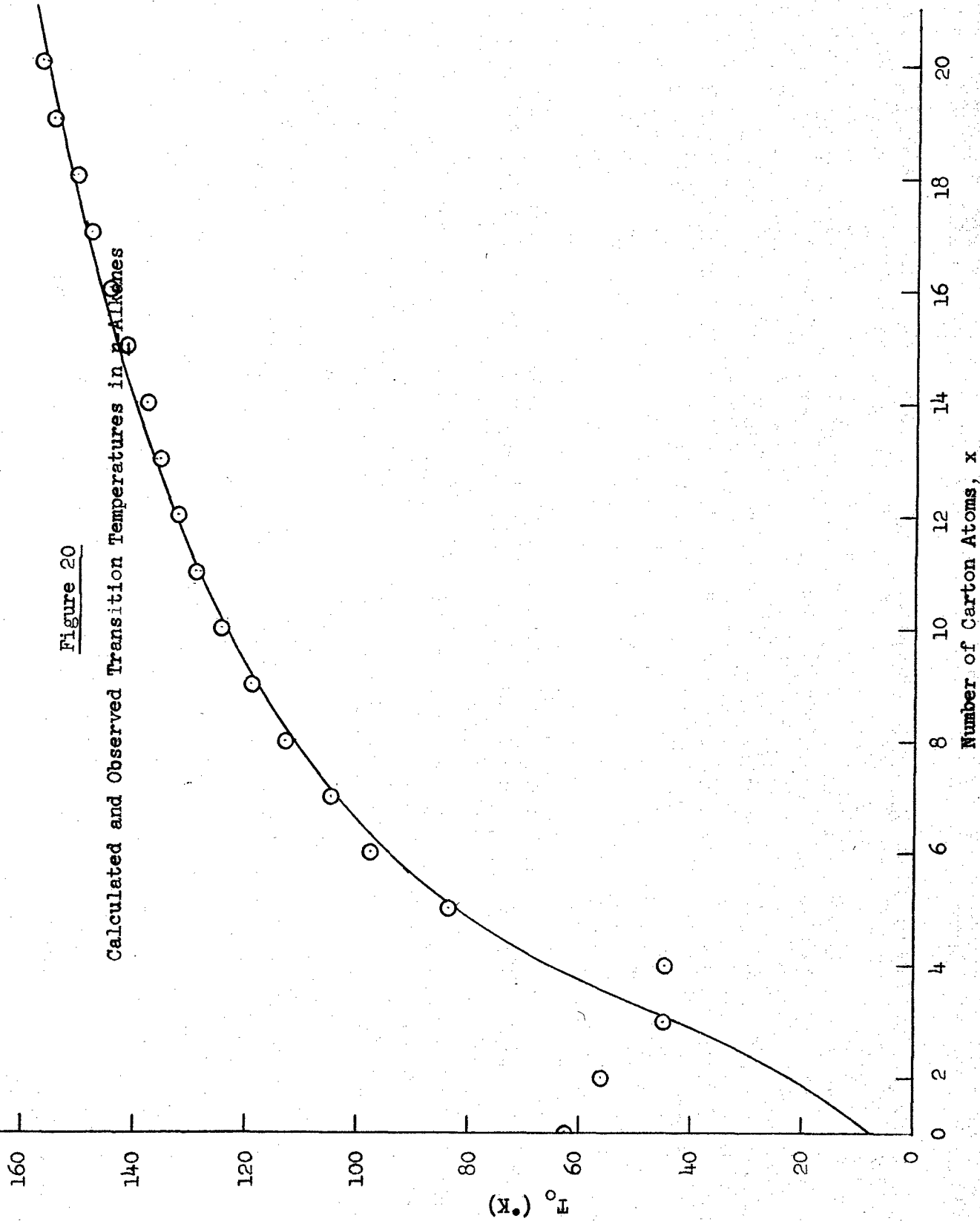
The estimated value of T_0 for $x \rightarrow \infty$ is 236.8°K, only slightly below a known transition in polyethylene.

C. Chain Bonds with Zero Flex Energy

The chain bonds in a polymethylene chain have one preferred conformation all others being of higher energy. This is probably true of vinyl polymers in general. However, structures can be conceived of which have chain bonds with two or more equivalent preferred conformers. That is, considering only the portions of the molecule immediately adjacent

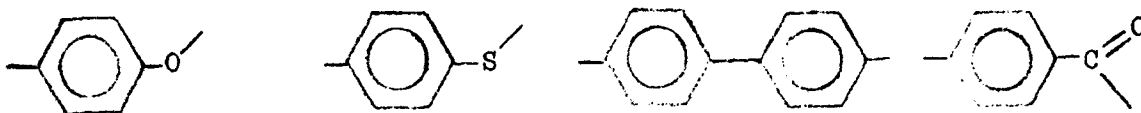
Figure 20

Calculated and Observed Transition Temperatures in Paraffines



to the bond in question, the lowest energy conformation may not be a unique structure, but may be repeated two or more times in a 360° rotation about that bond. For example, the C-O-C plane in anisole is rotated 22° with respect to the ring⁴⁹. The corresponding angle in diphenyl ether⁴⁹ is 37° and in diphenyl sulfide⁴⁹ 42° . Hence, the potential functions for rotation about the single bonds in these molecules must have four equal minima, at $\pm \phi$ and $180 \pm \phi$, where ϕ is the dihedral angle. Presumably, this type of rotational potential barrier results from a balance between steric effects, which favor the orthogonal conformation, and resonance effects, which favor the planar. The values above were estimated from dielectric measurements on solutions, but similar results are found for gases by electron diffraction studies and crystals by X-ray diffraction⁵⁰.

Non-planar conformations have also been reported for various substituted biphenyls⁵⁰ ($\phi = 45$ to 79°), aromatic acids⁵¹ ($\phi = 7$ to 65°), nitro-aromatic compounds⁵¹ ($\phi = 7$ to 49°), polyphenyls⁴⁹ ($\phi = 20$ to 55°), 1- and 2-methoxynaphthalene⁴⁹, 1- and 2-acetylnaphthalene⁴⁹, 1,4- and 1,5-dimethoxynaphthalene⁴⁹ ($\phi = 30^\circ$), 9,10-dimethoxyanthracene⁴⁹ ($\phi = 60^\circ$), benzophenone⁴⁹ ($\phi = 40^\circ$), and 2,2'-bipyridyl⁴⁹ ($\phi = 10$ to 17°). In general, therefore, we can expect to find four equal low energy conformers in all bonds of the following types:



If the rings are unsymmetrically substituted, two pairs of conformers should exist, differing in energy by some amount ϵ .

The Gibbs-DiMarzio theory as formulated in Equation (33) applies to chains in which all chain bonds are equivalent, and each has a single preferred conformation and $m-1$ higher-energy conformers. The theory can readily be generalized to encompass chains having bonds with two or more preferred conformers. Polymers of this kind usually have more than one type of bond in the chain, so that the theory must be expressed in copolymer form.

Consider a chain comprised of a rotatable bonds having m conformers of energy ϵ_k and b rotatable bonds having n conformers of energy ϵ_1 . The intramolecular energy can be partitioned into contributions from each type of bond:

$$E_i = \sum_k a_k \epsilon_k + \sum_l b_l \epsilon_l \quad (36)$$

Hence, from Equation (30),

$$\sum_i \exp(-E_i/RT) = \frac{1}{2} \left[\sum_{k=1}^m \exp(-\epsilon_k/RT) \right]^a + \frac{1}{2} \left[\sum_{l=1}^n \exp(-\epsilon_l/RT) \right]^b \quad (37)$$

If the chains are long enough so that we may neglect the term $x^{-1} \ln \frac{1}{2}$,

$$x^{-1} \ln \sum_i \exp(-E_i/RT) = \frac{a}{x} \ln \sum_{k=1}^m \exp(-\epsilon_k/RT) + \frac{b}{x} \ln \sum_{l=1}^n \exp(-\epsilon_l/RT) . \quad (38)$$

x is defined as the number of "backbone units" per chain, where each backbone unit occupies one lattice site. Each polymer chain may be characterized by the mole fraction of rotatable bonds of each type, x_1 , and by the ratio of lattice site occupiers to rotatable bonds, r :

$$r = x/(a + b + \dots) . \quad (39)$$

Equation (38) may now be written

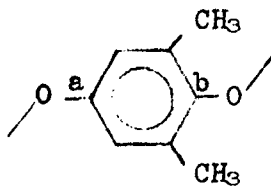
$$x^{-1} \ln \sum_i \exp(-E_i/RT) = \frac{x_a}{r} \ln \sum_{k=1}^m \exp(-\epsilon_k/RT) + \frac{x_b}{r} \ln \sum_{l=1}^n \exp(-\epsilon_l/RT) . \quad (40)$$

The relation for configurational entropy as a function of temperature, lattice parameters, and parameters characteristic of the polymer, analogous to Equation (33), follows immediately from the above considerations. A long-chain approximation is made to simplify the expression:

$$\begin{aligned}
 S_1/Rxn_x = & \frac{z-2}{2} \ln \left[1 - \frac{2(1-V_0)}{z} \right] + \frac{V_0(Xz)}{(1-V_0)2RT} \left[1 + \frac{zV_0}{(z-2)(1-V_0)} \right]^{-2} \\
 & + \frac{x_a}{r} \ln [m_0 + (m-m_0) \exp (-\epsilon_a/RT)] + \frac{x_b}{r} \ln [n_0 + (n-n_0) \exp (-\epsilon_b/RT)] \\
 & + \frac{1}{rRT} \left[\frac{x_a \epsilon_a \exp (-\epsilon_a/RT)}{m_0 + (m-m_0) \exp (-\epsilon_a/RT)} \right. \\
 & \left. + \frac{x_b \epsilon_b \exp (-\epsilon_b/RT)}{n_0 + (n-n_0) \exp (-\epsilon_b/RT)} \right]. \tag{41}
 \end{aligned}$$

In Equation (41), the summations have been evaluated assuming there are m_0 conformers of zero (relative) energy and $m-m_0$ conformers of identical energy ϵ .

To illustrate the application of Equation (41) to the estimation of glass temperature let us consider the 1,4-polyether of 2,6-xyleneol:



The two rotatable bonds in the repeat unit, labeled a and b, are of the type which have four equally preferred conformers, as discussed above. Hence $m = m_0 = n = n_0 = 4$ and $\epsilon_a = \epsilon_b = 0$. Since bonds a and b are collinear, their rotations are correlated in such a way that there are only eight distinguishable conformers for the pair. We can therefore treat this polymer as a one-bond chain with $m = m_0 = 8$. Notice that

each bond contributes $(R/r) \ln 8$ to the configurational entropy, independent of temperature. The transition in this type of chain arises entirely from the temperature dependence of the intermolecular contribution.

The interaction energy α can be calculated from the values of $(E-V)^{1/2}$, given by Small⁵²: $C_6H_2 = 488$, $CH_3 = 214$ and $O = 70$. The molecular weight of the repeat unit is 120.144, the polymer density is 1.0653 and the number of lattice site occupiers in the repeat unit is r . Hence

$$\alpha = \frac{-(986)^2 (1.06)}{120.144 \times r} = \frac{-8,577}{r} \text{ cal. mole}^{-1} \quad (42)$$

Inserting this value of α in Equation (41) with $z = 6$, $V_0 = 0.04$, and $S_1 = 0$, we have

$$0 = -0.77132 + 0.027860 (-8,577)/r T_2 + r^{-1} \ln 8. \quad (43)$$

A DTA analysis of a sample of PPO C1001, which is the General Electric Company's designation for a molding grade polymer of this type, showed a glass transition at 207°C. Assuming that this polymer has a normal value of $T_g - T_2 = 55^{\circ}$, then $T_2 = 425^{\circ}$. Hence from Equation (43), a value of 1.967 lattice site occupiers in the repeat unit is required for perfect agreement with the observed glass temperature. This quantity is probably correlated with the size of the constituent groups that make up the repeat unit, but such a correlation has not yet been developed.

4. Transition State Theory and the Glass Transition

It was shown in the summary report of July 1965⁵ that an expression based on the Fulcher equation accurately describes the temperature dependence of dielectric relaxation times in several polymers. The expression,

$$\log \tau = \log A - \log T + \frac{B}{T-T_0}, \quad (44)$$

was chosen to correspond to the form of the Eyring rate equation^{54,55}

$$\log \tau = \log \frac{h}{Kk} - \log T + \frac{\Delta G^\ddagger}{2.303 RT}. \quad (45)$$

The free energy term $\Delta G^\ddagger/2.303 RT$ is given by $B/(T-T_0)$ if the reasonable assumption is made that the transmission coefficient K remains constant over the temperature range of interest. It has been amply demonstrated that the form $B/(T-T_0)$ is an excellent representation of the temperature dependence of the activation energy (or free volume) in liquid transport processes^{1-5,11}.

Best-fit values of A , B , and T_0 were computed using least-square methods from published dielectric relaxation data¹⁶ on PMMA, PEMA, PBMA, PVAc and PVC.

The computed values of $\log A$ were relatively close to the theoretical value of $\log (h/k)$, which is -10.32 , as Reference 5 indicates.

This result suggested that the data be tested with an equation of the form,

$$\log \tau = \log \frac{h}{k} - \log T + \sum_{i=1}^n \frac{B_i}{(T-T_0)^i}, \quad (46)$$

wherein additional terms in powers of $1/T-T_0$ may be added to improve the accuracy.

When terms through the second order are retained in the expansion of Equation (46), the following equation results:

$$\log \tau = \log \frac{h}{k} - \log T + \frac{B}{T-T_0} + \frac{C}{(T-T_0)^2} \quad (47)$$

Equation (47) has three adjustable parameters, as does Equation (44). Thus, an adequate test of Equation (47) is to compare it with Equation (44). With this in mind, the Mathematical Analysis Group was requested to fit Equation (47) to Saito's¹⁶ dielectric data.

The results indicated that Equation (47) fits the data about as well as Equation (44), according to the variance estimates obtained for the least-squares fits. The variance results are given in Table VII.

The calculation of the transition state parameters was more revealing. The following expressions were used to calculate ΔG^\ddagger , ΔH^\ddagger , and ΔS^\ddagger at the glass temperature:

$$\Delta G^\ddagger = 2.303 RT \left[\frac{B}{T_g - T_0} + \frac{C}{(T_g - T_0)^2} \right] \quad (48)$$

$$\Delta H^\ddagger = \frac{2.303 RT^2}{T_g - T_0} \left[\frac{B}{T_g - T_0} + \frac{2C}{(T_g - T_0)^2} \right] \quad (49)$$

$$\Delta S^\ddagger = \frac{\Delta H^\ddagger - \Delta G^\ddagger}{T_g} \quad (50)$$

The results are shown in Table VIII. The ΔG^\ddagger values obtained with Equation (44) are shown for comparison.

It is apparent from examination of Table VIII that the G^\ddagger values are much less scattered for a given polymer when based on Equation (47). Since one would not normally expect a great deal of scatter in ΔG^\ddagger , this is a reasonable indication that Equation (47) is superior to Equation (44). This, of course, amounts to a sort of experimental confirmation of Eyring's transition state theory^{54,55} as applied to dielectric relaxation.

TABLE VII

Equation (47) Results and Comparison of Variance
Estimates Obtained with Equations (44) and (47)

Polymer	$M_{vis} \times 10^4$	B	C	T_0	Variance Est. $\times 10^4$	
					Eq. (47)	Eq. (44)
PBMA	-	1337.4	-2.964×10^3	186.8	17.7	5.4
PEMA	-	1156.7	14.42	251.8	17.9	8.9
PMMA	110	549.9	1.424×10^4	324.7	1.61	1.5
	54	322.5	5.796×10^4	302.2	25.4	26.4
	33	608.1	1.920×10^2	332.6	14.0	11.2
	15	279.3	7.068×10^4	291.5	3.65	3.1
	8.5	313.3	6.298×10^4	290.5	7.4	6.5
PVC	17.4	331.7	3.686×10^4	293.7	15.8	17.5
	10.1	98.0	8.000×10^4	277.6	6.5	7.1
	7.6	93.9	8.401×10^4	274.2	2.9	3.0
	5.8	24.7	9.854×10^4	268.6	3.1	3.4
	4.57	162.3	7.314×10^4	274.0	0.24	0.12
PVAc	3.62	39.0	9.699×10^4	266.1	3.6	2.9
	52.3	730.5	1.866×10^2	261.4	7.7	7.6
	26.1	719.1	5.158×10^2	261.6	35.3	25.9
	18.8	722.2	3.275×10^2	260.8	21.2	16.2
	11.2	720.6	4.780×10^3	255.9	9.0	8.8
	3.95	720.1	1.312×10^2	261.0	40.3	31.2

TABLE VIII

Transition State Parameters at the Glass Temperature
Computed with Equations (48), (49), and (50)

<u>Polymer</u>	<u>Mvis x 10⁴</u>	<u>ΔG^\ddagger, kcal.</u>		<u>ΔH^\ddagger, kcal.</u>	<u>ΔS^\ddagger, eu</u>	
		<u>Eq. (48)</u>	<u>Eq. (49)</u>			
PBMA	-	16.5	14.9	47	102	
PEMA	-	24.0	21.3	109	262	
PMMA	110	25.3	26.4	228	534	
	54	25.2	28.8	216	506	
	33	25.5	24.2	233	557	
	15	24.6	29.0	201	474	
	8.5	25.4	29.6	212	509	
	PVC	17.4	22.7	25.1	204	506
		10.1	22.7	27.2	194	480
7.6		22.3	26.8	185	457	
5.8		22.3	27.6	182	452	
4.57		22.1	26.0	182	451	
3.62		22.1	26.9	178	444	
PVAc	52.3	23.9	23.9	169	476	
	26.1	24.3	23.6	179	511	
	18.8	23.9	23.3	173	490	
	11.2	24.7	24.3	182	518	
	3.95	24.3	23.3	179	512	

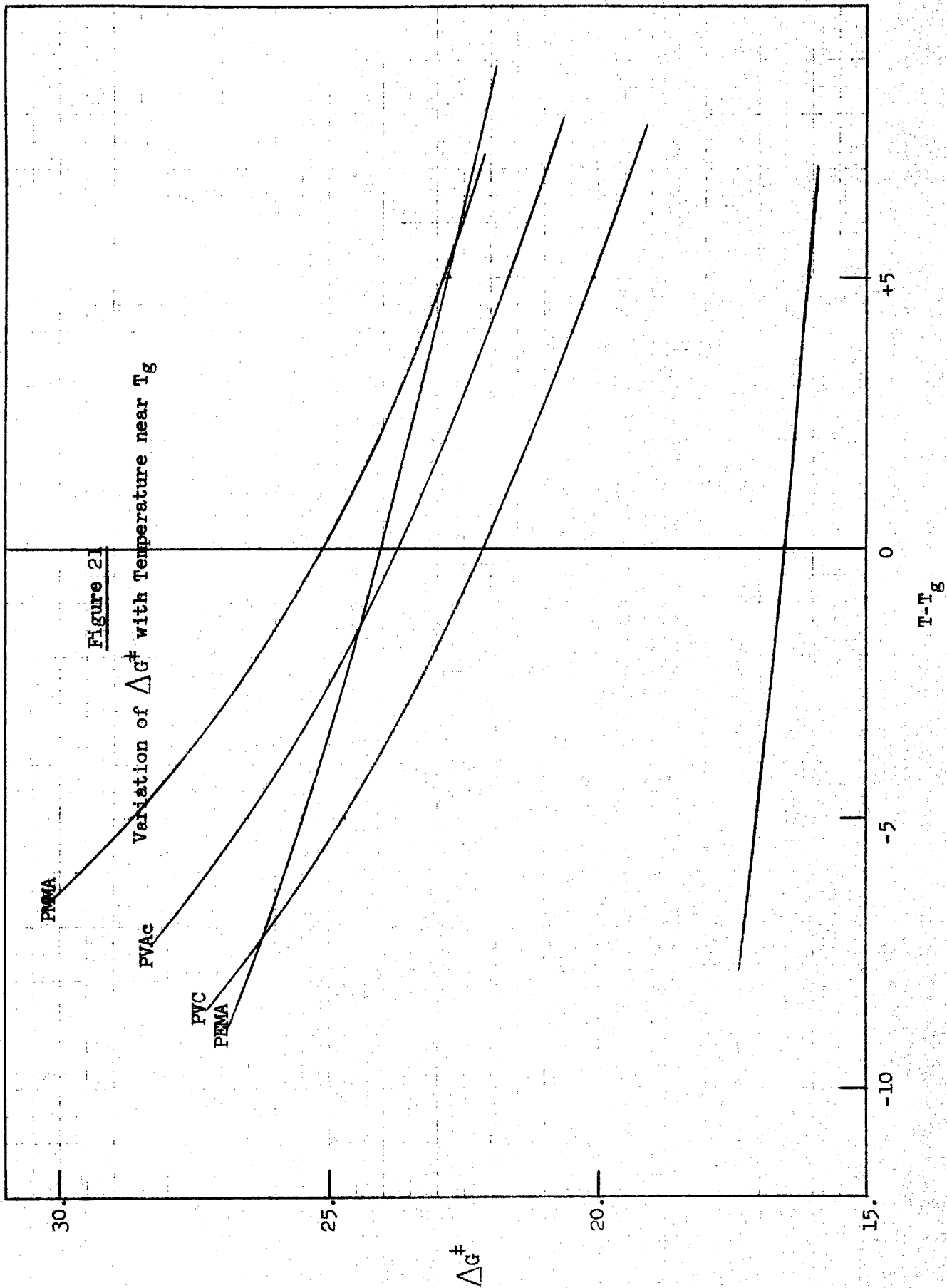
Earlier in this program it was suggested that a condition for the glass temperature might be a value of ΔG^\ddagger near 25 kcal. Table VIII indicates that this is not the case. However, if ΔG^\ddagger were extremely temperature sensitive around the glass temperature, it still might be possible to obtain an approximate value of T_g by finding the temperature at which ΔG^\ddagger has some arbitrary value, using Equation (47). To test this, values of ΔG^\ddagger were calculated for the polymers under consideration in the range $T_g - 5^\circ \leq T \leq T_g + 5^\circ$. The result is shown graphically in Figure 21. Although a value of ΔG^\ddagger at T_g of 24 kcal. would be excellent for PEMA, PMMA, PVC, and PVAc, the same value would result in a large error in predicting T_g for PBMA.

This PBMA anomaly may have as its underlying cause the rather unusual relaxation behavior of the methacrylates. In these polymers, dynamic measurements made at temperatures just above T_g show that as the length of the side group increases, the α and β dispersion regions come together⁵⁶. The fusion of the two regions is essentially complete in PBMA, so that only one loss peak is observed for both processes. It is well known that the β dielectric loss peak is much larger than the α peak in the lower methacrylate atactic and syndiotactic polymers^{16,56,58}. Thus, the characteristics of the loss peak in PBMA are more likely to reflect the unresolved β process than the α process, and we cannot expect meaningful results if this peak is viewed as the α loss peak. In fact, Saito's¹⁶ results extrapolate to a relaxation time of less than 2 seconds at the glass temperature, which is certainly an unreasonably small value.

If one assumes that the glass transition is characterized by a fixed relaxation time for a given set of experimental conditions (as expanded in Part II of this report), then transition state theory leads to a condition for T_g other than constant ΔG^\ddagger . Equation (45) may be written in the form

$$\frac{\Delta G_g^\ddagger}{T_g} = 2.303 R \left(\log \tau_g - \log \frac{h}{k} + \log T_g \right) . \quad (51)$$

If we vary T_g from 270°K to 380°K, $\log T_g$ will lie in a small interval, 2.43 to 2.58. This amounts to a variation of only + 0.08 in $(\log \tau - \log h/k + \log T)$ which has a value of about 15.8, i.e. less than a one per cent variation in $\Delta G^\ddagger/T_g$. This gives us a "universal" condition for the glass temperature. Nominally taking a relaxation time of 1000 seconds at T_g , we will obtain



$$\frac{\Delta G_g^\ddagger}{T_g} = 72.4 \pm 0.08 . \quad (52)$$

Let us see how well this expression works. First, we will calculate ΔG_g^\ddagger and $\Delta G_g^\ddagger/T_g$ at the observed dilatometric glass temperature using Equation (48). The results are shown in Table IX.

The next step is the calculation of ΔG_g^\ddagger and $\Delta G_g^\ddagger(\tau)/T_g(\tau)$ with T_g equal to 1000 seconds. This is done using Equations (47) and (48). These results are also given in Table IX.

As the Table indicates, the experimental values of ΔG_g^\ddagger and $\Delta G_g^\ddagger/T_g$ exhibit much scatter, as indicated by the fractional variance and standard deviation. After imposing the fixed relaxation time condition, $\Delta G_g^\ddagger(\tau)$ shows a slight increase in the fractional variance, but $\Delta G_g^\ddagger(\tau)/T_g(\tau)$ is now almost perfectly constant.

A glance at Equation (47) and (48) shows that the nearly perfect constancy of $\Delta G_g^\ddagger(\tau)/T_g(\tau)$ is a mathematical necessity. Significant deviation can occur only when the transition temperature is far from the nominal value selected here, about 325°K.

Another interesting aspect of this study is the difference between the dilatometric T_g and the dielectric T_g . Excluding the data on poly(n-butyl methacrylate) because of the unresolved α and β dispersions, we find that the T_g difference ranges from 1.9° to 6.5°. The average difference is 4.1°, with no consistent positive or negative trend in T_g (dilatometric) minus $T_g(\tau)$. This differential is certainly small compared to the over-all size of the transition region, and since the dilatometric transition temperature is itself chosen in a somewhat arbitrary fashion, it is quite possible that the dielectric and structural relaxation times of these polymers are equal.

Litovitz and his coworkers⁵⁹ have shown that in polar liquids wherein nonpolar regions make up large parts of the molecule, the dielectric relaxation time is much larger than the structural relaxation time. This is attributed to an increase in the entropy of activation for structural relaxation due to motions of nonpolar regions not coupled to dipoles. We have not found this relaxation time differential here, and therefore, in view of what Litovitz⁵⁹ has said, we conclude that the nonpolar regions of the polymers are effectively coupled to the dipoles.

TABLE IX

Values of ΔG_g^\ddagger and $\Delta G_g^\ddagger/T_g$ Computed before and after Reduction to Fixed Relaxation Time ($\tau_g = 10^3$ sec.)

Polymer	$M_{vis} \times 10^4$	Calculations Based on Dilatometric Results (Saito)			Calculations Based on $\tau_g = 10^3$ sec.		
		$T_g, ^\circ K$	$\Delta G_g^\ddagger, kcal$	$\Delta G_g^\ddagger/T_g, kcal deg^{-1}$	$T_g, ^\circ K$	$\Delta G_g^\ddagger, kcal$	$\Delta G_g^\ddagger/T_g, kcal deg^{-1}$
PBMA	-	289	16.5	58.5	269.3	19.4	72.0
PEMA	-	323	24.0	74.3	324.9	23.5	72.4
PMMA	110	380	25.3	66.6	276.6	27.4	72.7
	54	377	25.2	66.8	373.6	27.2	72.7
	33	374	25.5	68.2	371.2	27.0	72.7
	15	372	24.6	66.1	367.5	26.7	72.7
	8.5	366	25.4	69.4	364.1	26.5	72.6
PVC	17.4	359	22.7	63.2	353.5	25.7	72.6
	10.1	257	22.7	63.6	351.8	25.5	72.6
	7.6	356	22.3	62.6	350.0	25.4	72.6
	5.8	354	22.3	63.0	348.2	25.3	72.6
	4.6	353	22.1	62.6	347.2	25.2	72.6
	3.6	352	22.1	62.8	345.5	25.1	72.6
PVAc	52.3	304	23.9	78.6	307.8	22.3	72.3
	26.1	303	24.3	80.2	307.8	22.3	72.3
	18.8	303	23.9	78.9	307.0	22.2	72.3
	11.2	303	24.7	81.5	307.5	22.2	72.3
	4.0	302	24.3	80.5	306.8	22.2	72.3
Fractional Variance, $\sigma_x^2 / \langle x \rangle^2, \times 10^3$			6.25	11.3		8.11	0.02
Standard Deviation			1.85	7.38		2.21	0.32

This coupling reflects the size of the cooperative region. Since the dielectric data analyzed here were all obtained near the glass temperature, we would expect the cooperative region to be approaching its maximum size, and therefore it would be surprising if there were no evidence of coupling. At much higher temperatures the size of the cooperative region would be small, and we might anticipate a sizable difference between the structural and dielectric relaxation times.

References

1. M. L. Williams, R. F. Landel, and J. D. Ferry, *J. Am. Chem. Soc.*, 77, 3701 (1955).
2. M. H. Cohen and D. Turnbull, *J. Chem. Phys.*, 31, 1164 (1959).
3. F. Bueche, "Physical Properties of Polymers," Interscience Publishers, New York, 1962.
4. G. Adam and J. H. Gibbs, *J. Chem. Phys.*, 43, 139 (1966).
5. O. G. Lewis and L. V. Gallacher, "The Relationships between Polymers and Glass Transition Temperatures," Technical Report AF ML-TR-65-231, July 1965.
6. D. Robertson and K. A. Walch in "Temperature, Its Measurement and Control in Science and Industry," Vol. 3, Part 1, F. G. Brickwedde, Ed., Reinhold, New York, 1962. Chapter 32.
7. M. R. Cannon, R. E. Manning, and J. D. Bell, *Anal. Chem.*, 32, 355 (1960).
8. Experimental methods and detailed descriptions of most standard glass capillary viscometers are found in ASTM D-445-1P71. Appendices C and N of this section describe the viscometers used here.
9. See, for example: J. R. VanWazer, J. W. Lyons, K. Y. Kim, and R. E. Colwell, "Viscosity and Flow Measurement," Interscience, New York, 1963. Chapter 4.
10. R. S. Porter and J. F. Johnson, *Chem. Rev.*, 66, 1 (1966).
11. G. S. Fulcher, *J. Am. Ceram. Soc.*, 8, 339 (1925).
12. P. Heydemann and H. D. Guicking, *Kolloid-Z.*, 193, 16 (1963).
13. B. Wunderlich and D. M. Bodily, *J. Appl. Phys.*, 35, 103 (1964).
14. H. Martin and F. H. Muller, *Makromol. Chem.*, 75, 75 (1964).
15. T. Holt and D. Edwards, *J. Appl. Chem.*, 15, 223 (1965).
16. S. Saito, "Study of Molecular Motions in Solid Polymers by the Dielectric Measurements," No. 648, Researches of the Electrotechnical Laboratory, Agency of Industrial Science and Technology, Japan, 1964; also, S. Saito, *Kolloid-Z.*, 189, 116 (1963).
17. For a comprehensive review of dynamic mechanical results, see A. E. Woodward and J. A. Sauer in "Physics and Chemistry of the Organic Solid State," Vol. 2, D. Fox, M. M. Labes, and A. Weissberger, Eds., Interscience Publishers, New York, 1965.

18. B. Wunderlich and D. M. Bodily, *J. Polymer Sci.C*, 6, 137 (1964).
19. G. P. Mikhailov and T. I. Borisova, *Vysokomol. Soedin.*, 2, 619 (1960).
20. A. J. Curtis in "Progress in Dielectrics," Vol. 2, J. B. Birks, Ed., John Wiley and Sons, New York, 1960.
21. R. F. Boyer, *Rubber Chem. Tech.*, 36, 1303 (1963).
22. G. E. McDuffie, Jr., and T. A. Litovitz, *J. Chem. Phys.*, 37, 1699 (1962).
23. See, for example, J. D. Ferry, and S. Strella, *J. Colloid Sci.*, 13, 459 (1958).
24. Y. Ishida, *Kolloid-Z.*, 168, 29 (1960).
25. Y. Ishida and K. Yamafuji, *Kolloid-Z.*, 177, 97 (1961).
26. F. E. Karasz, H. E. Bair, and J. M. O'Reilly, *J. Phys. Chem.*, 69, 2657 (1965).
27. See, R. C. Reid and T. K. Sherwood, "The Properties of Gases and Liquids," McGraw-Hill, New York, 1958, Chapter 3.
28. See, for example, A. J. Kovacs, *Fortschr. Hochpolymer Forsch.*, 3, 394 (1963).
29. N. Hirai and H. Eyring, *J. Polymer Sci.*, 37, 51 (1959).
30. T. Alfrey, G. Goldfinger and H. Mark, *J. Appl. Phys.*, 14, 700 (1943).
31. R. S. Spencer and R. F. Boyer, *J. Appl. Phys.*, 17, 398 (1946).
32. R. S. Spencer, *J. Colloid Sci.*, 4, 229 (1949).
33. A. J. Kovacs, *J. Polymer Sci.*, 30, 131 (1958). Also see J. D. Ferry, "Viscoelastic Properties of Polymers," John Wiley and Sons, New York, 1961, Chapter 18.
34. W. Sommer, *Kolloid-Z.*, 167, 97 (1959).
35. T. G. Fox and P. J. Flory, *J. Appl. Phys.*, 21, 581 (1950).
36. See, for example, W. A. Weyl and E. C. Marboe, "The Constitution of Glasses, A Dynamic Interpretation," Interscience Publishers, New York, 1964, Chapter 19.
37. P. L. Kirby in "Non-Crystalline Solids," V. D. Frechette, Ed., John Wiley and Sons, New York, 1960.

38. A. Q. Tool, J. Am. Ceram. Soc., 29, 240 (1946).
39. H. N. Ritland, J. Am. Ceram. Soc., 37, 370 (1954).
40. E. N. da C. Andrade, "Viscosity and Plasticity," Chemical Publishing Co., New York, 1951.
41. G. M. Martin, S. S. Rogers, and L. Mendelkern, J. Polymer Sci., 20, 579 (1956).
42. J. H. Gibbs and E. A. DiMarzio, J. Chem. Phys., 28, 373 (1958).
43. A. K. Doolittle, J. Appl. Phys., 22, 1471 (1951).
44. P. J. Flory, Proc. Royal Soc. (London), A234, 60 (1956).
45. E. A. DiMarzio and J. H. Gibbs, J. Chem. Phys., 28, 807 (1958).
46. E. A. DiMarzio and J. H. Gibbs, J. Polymer Sci., 40, 121 (1959).
47. E. A. DiMarzio and J. H. Gibbs, J. Polymer Sci. A, 1, 1417 (1963).
48. O. G. Lewis, J. Chem. Phys., 43, 2693 (1965).
49. R. J. W. LeFevre in "Advances in Physical Organic Chemistry," 3, V. Gold, Ed., Academic Press, N. Y., 1965.
50. L. L. Ingraham in "Steric Effects in Organic Chemistry," M. S. Newman, Ed., John Wiley and Sons, Inc., N. Y., 1956.
51. G. Ferguson and J. M. Robertson in "Advances in Physical Organic Chemistry," 1, V. Gold, Ed., Academic Press, N. Y., 1963.
52. P. A. Small, J. Appl. Chem. (London), 3, 71 (1953).
53. Technical Bulletin, General Electric Company.
54. S. Glasstone, K. J. Laidler, and H. Eyring, "The Theory of Rate Processes," McGraw-Hill Book Co., Inc., N. Y., 1941.
55. W. Kauzmann, Revs. Mod. Phys., 14, 12 (1942).
56. N. S. Steck, SPE Trans., 4, 34 (1964).
57. M. E. Baur and W. H. Stockmayer, J. Chem. Phys., 43, 4319 (1965).
58. G. P. Mikhaelov and T. I. Borisova, Polymer Sci. (USSR), 2, 387 (1961).
59. See, for example, T. A. Litovitz in "Non-Crystalline Solids," V. D. Frechette, Ed., John Wiley and Sons, Inc., N. Y., 1960.